



Contents lists available at ScienceDirect

# Modeling of naphtha reforming unit applying detailed description of kinetic in continuous catalytic regeneration process

Davood Iranshahi<sup>a,c</sup>, Mohsen Karimi<sup>a</sup>, Shahram Amiri<sup>a</sup>, Mitra Jafari<sup>a</sup>, Razieh Rafiei<sup>a</sup>, Mohammad Reza Rahimpour<sup>a,b,\*</sup>

<sup>a</sup> Dept. of Chemical Engineering, School of Chemical and Petroleum Engineering, Shiraz University, Shiraz 71345, Iran

<sup>b</sup> Department of Chemical Engineering and Materials Science, University of California, Davis, 1 Shields Avenue, Davis, CA 95616, United States

<sup>c</sup> Department of Chemical Engineering, Amirkabir University of Technology, Tehran, Iran



CrossMark

## ABSTRACT

Naphtha reforming is one of the most important processes in refineries in which high value-added reformate for gasoline pool and aromatics such as benzene, toluene, and xylene are produced. It is necessary to establish new naphtha reforming units and develop the traditional units to increase the efficiency of the processes. In this study, according to the recent progresses in the naphtha reforming technology, mathematical modeling of this process in continuous catalyst regeneration mode of operation is accomplished in two dimensions (radial and axial) by considering cross flow pattern. In addition, a new catalyst deactivation model has been proposed and a new reaction network model based on 32 pseudo-components with 84 reactions is investigated. Then, this model has been validated by comparing with industrial data, and its results have acceptable agreement.

© 2013 The Institution of Chemical Engineers. Published by Elsevier B.V. All rights reserved.

**Keywords:** Catalytic naphtha reforming process; Continuous catalytic regeneration; Two dimensional mathematical modeling; Reaction network; Catalyst deactivation model.

## 1. Introduction

Naphtha reforming process is one of the key processes in petroleum refining for providing high value-added reformate for the gasoline pool. It is also used for producing BTX (benzene, toluene, and xylene) by conversion of paraffins and naphthenes to aromatics-rich products which are the basic substances of the petrochemical processes. Hydrogen is also considered as a main by-product and in the most refineries is used in hydrocracking, hydrotreating, and other hydrogen consuming reactions (Aitani, 2005a,b; Antos and Aitani, 1995; Hongjun et al., 2010). Full-range naphtha is the fraction of the crude oil with a boiling temperature between 30 and 200 °C, and constitutes typically 15–30 wt% of the crude oil (Antos and Aitani, 1995). Based on the mode of catalyst regeneration, the reforming process is generally classified into three types:

1. Semi regenerative.
2. Cyclic.
3. Continuous regenerative (moving bed).

As shown in Fig. 1, 60% of total capacity of reforming process is the semi regenerative scheme, while the continuous regeneration and the cyclic have 28% and 12% of total capacity of reforming, respectively (Antos and Aitani, 1995). Today, due to many benefits of continuous regeneration, all new units are designed based on this technology and old units are revamped to the continuous regeneration process or are combined with this process. There are some advantages of CCR process against traditional methods, such as producing higher octane reformate even working with a low feed quality, long time working of the process due to lack of shut down, operating in the lower pressure by the low pressure drop,

\* Corresponding author at: Dept. of Chemical Engineering, School of Chemical and Petroleum Engineering, Shiraz University, Shiraz 71345, Iran. Tel.: +98 711 2303071; fax: +98 711 6287294.

E-mail addresses: [rahimpur@shirazu.ac.ir](mailto:rahimpur@shirazu.ac.ir), [mrahimpour@ucdavis.edu](mailto:mrahimpour@ucdavis.edu) (M.R. Rahimpour).

Received 26 April 2013; Received in revised form 11 September 2013; Accepted 14 December 2013

0263-8762/\$ – see front matter © 2013 The Institution of Chemical Engineers. Published by Elsevier B.V. All rights reserved.

<http://dx.doi.org/10.1016/j.cherd.2013.12.012>

**Notation**

$a_i$	catalyst activity
$a_A$	acidic function activity
$a_{C_A}$	acidic function activity for coke formation
$a_{C_M}$	metallic function activity for coke formation
$a_M$	metallic function activity
$A_r$	cross-section area of reactor in radial direction, m <sup>2</sup>
$C$	concentration, kmol m <sup>-3</sup>
$C_{ACP}$	alkyl-cyclopentane concentration, kmol m <sup>-3</sup>
$C_{CA}$	coke weight fraction on acidic function of catalyst, kg kg <sup>-1</sup>
$C_{CM}$	coke weight fraction on metallic function of catalyst, kg kg <sup>-1</sup>
$C_{j0}$	inlet concentration of component j, kmol m <sup>-3</sup>
$C_p$	specific heat capacity at constant pressure, kJ kmol <sup>-1</sup> K <sup>-1</sup>
$C_v$	specific heat capacity at constant volume, kJ kmol <sup>-1</sup> K <sup>-1</sup>
$C_T$	total concentration, kmol m <sup>-3</sup>
$d_p$	particle diameter, m
$D_e$	effective diffusivity, m <sup>2</sup> s <sup>-1</sup>
$E_c$	coke formation activation energy, J mol <sup>-1</sup>
$F$	molar flow rate, kmol h <sup>-1</sup>
$F_j$	molar flow rate of component j, kmol h <sup>-1</sup>
$F_t$	total molar flow rate to the reactor, kmol h <sup>-1</sup>
$H$	enthalpy, J mol <sup>-1</sup>
$H_j$	enthalpy of component j, J mol <sup>-1</sup>
$k$	thermal conductivity, W m <sup>-1</sup> K <sup>-1</sup>
$k_{CA}$	constant of deactivation equation for acidic function, kg kg <sup>-1</sup> kPa <sub>1</sub> <sup>n</sup> m <sup>1.5</sup> kmol <sup>-1.5</sup>
$k_{CM}$	constant of deactivation equation for metallic function, kg kg <sup>-1</sup> kPa <sub>1</sub> <sup>n</sup> m <sup>1.5</sup> kmol <sup>-1.5</sup>
$k_{eff}$	effective thermal conductivity, W m <sup>-1</sup> k <sup>-1</sup>
$k_{in}$	reaction rate constant for reaction
$K_{in}$	equilibrium constant for reaction
$L$	length of reactor, m
$m$	number of reactions
$M_j$	molecular weight of component j, kg kmol <sup>-1</sup>
$M$	mean molecular weight in the flow, kg kmol <sup>-1</sup>
$n$	number of components
$n_1$	constant of deactivation equation
$n_2$	constant of deactivation equation
$n_A$	acidic function activity power number
$n_{CA}$	acidic function activity power number
$n_M$	metallic function activity power number
$n_{CM}$	metallic function activity power number
$N_j$	molar flux of component j, kmol m <sup>-2</sup> h <sup>-1</sup>
$P$	total pressure, kPa
$P_{An}$	partial pressure of aromatic with n carbon, kPa
$P_{ACH_n}$	partial pressure of alkyl-cyclohexane with n carbon, kPa
$P_{ACP_n}$	partial pressure of alkyl-cyclopentane with n carbon, kPa
$P_{H_2}$	partial pressure of hydrogen, kPa
$P_{IP_n}$	partial pressure of iso-paraffin with n carbon, kPa
$P_{NP_n}$	partial pressure of normal-paraffin with n carbon, kPa
$r$	radius, m
$r_i$	rate of ith reaction, kmol kg cat <sup>-1</sup> h <sup>-1</sup>

 $r_{in}$  rate of inth reaction, kmol kg cat<sup>-1</sup> h<sup>-1</sup> $r_C^0$  rate of coke formation on fresh catalyst, kg kg cat<sup>-1</sup> h<sup>-1</sup> $r_{CA}$  rate of coke formation on acidic function of catalyst, kg kg cat<sup>-1</sup> h<sup>-1</sup> $r_{CM}$  rate of coke formation on metallic function of catalyst, kg kg cat<sup>-1</sup> h<sup>-1</sup> $R$  gas constant, J mol<sup>-1</sup> K<sup>-1</sup> $R_i$  inner diameter, m $R_o$  outer diameter, m $S_a$  specific surface, m<sup>2</sup> g<sup>-1</sup> $T$  temperature, K $U$  overall heat transfer coefficient, W m<sup>-2</sup> K<sup>-1</sup> $U_j$  internal energy of component j $u_r$  radial velocity, m s<sup>-1</sup> $y_j$  mole fraction of component (j)**Greek letters** $\varepsilon$  void fraction of catalyst bed $\mu$  viscosity, kg m<sup>-1</sup> s<sup>-1</sup> $v_{ij}$  stoichiometric coefficient of component j in reaction i $\rho_b$  reactor bulk density, kg m<sup>-3</sup> $\phi_s$  sphericity, $\Delta H$  heat of reaction, kJ mol<sup>-1</sup> $\Delta z$  control volume length, m $\Delta r$  control volume thickness in radial direction, m $\alpha_A$  constant of deactivation, m<sup>3</sup> kmol<sup>-1</sup> $\alpha_{CA}$  constant of deactivation, m<sup>3</sup> kmol<sup>-1</sup> $\alpha_{CM}$  constant of deactivation, m<sup>3</sup> kmol<sup>-1</sup> $\pi$  Pi number, 3.14156 $\alpha_M$  constant of deactivation, m<sup>3</sup> kmol<sup>-1</sup>**Subscript** $e$  exit condition $i$  numerator for reaction $j$  numerator for component $n$  number of carbon atom $T$  total**Abbreviations**

A aromatics

ACH alkyl-cyclohexane

ACP alkyl-cyclopentane

CCR continuous catalyst regeneration reformer

F scaling factor

HC hydrocarbon

IBP initial boiling pint, °C

IP iso-paraffin

NP normal-paraffin

RON research octane number

Pt platinum

Sn tin

using catalyst with less stability but higher selectivity and yield, requiring lower recycle ratio, economic design, producing more reformate with higher aromatic content and steady production of hydrogen with constant purity (93% compared to 80% in the semi regenerative process) (Aitani, 2005a,b; Antos and Aitani, 1995; Hongjun et al., 2010; Edgar, 1983; Lee et al., 1997). In addition, the deposited coke in the semi regenerative

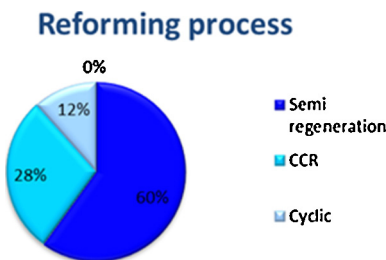


**Fig. 1 – Capacity of different types reforming process in the world.**

reformer can be varied from a few weight percent on the first reactor to 20 wt% coke in the last reactor. In the cyclic regenerative reformers, catalyst regeneration is usually based on economics performance for one or more of the reactors in the reforming process loop. While in the CCR process that operates with a platinum/tin catalyst, the deposited coke on the catalyst is usually restricted to less than 7 wt% in the last reactor (Antos and Aitani, 1995). Thus, according to these advantages of CCR process the capacity of the CCR reforming units has increased quickly in the recent years. Generally, the naphtha reforming unit consists of four reactors, catalyst regeneration unit, distillation column which separates products into light hydrocarbons and reformates, and due to endothermic reactions in the reforming process, inlet stream to each reactor is preheated via a furnace.

Accomplished researches regard naphtha reforming process could be classified in three categories. The first category consists of the accomplished studies on kinetic models of catalytic naphtha reforming. To reduce the complexity of the reaction system, similar chemical components are lumped together and represented as a pseudo component, and the reactions among the pseudo components are considered (Hongjun et al., 2010). Primary studies about lumped kinetic have been done by Smith (1959), Krane et al. (1959) Kmak (1972), Ramage et al. (1980), Wolff and Kramarz (1979) and Jenkins and Stephens (1980). To satisfy various demands on the reforming process, different pseudo components have been considered in the proposed network kinetic models. Marin et al. (1983) and Froment (1987) published the reaction network for the whole range of naphtha reforming. In addition, by considering this fact that the reaction pathways derived for each carbon number fraction are almost identical to each other, Ramage et al. (1987) used the same reaction network within each carbon number group. Jorge and Eduardo (2000) proposed a 24 lumps model in order to model the kinetic of catalytic naphtha reforming reactions. Hu et al. (2003) proposed kinetic model with 17-lump while Weifeng et al. (2006) proposed kinetic model with 18-lumpes. The second class of studies have been focused on improving the operation and selectivity of the catalyst and reduce the probability of coke formation on the catalyst surface by adding some metals such as Sn, In, and Ge to the catalyst. The literature survey about these concepts is discussed extensively in previous work (Iranshahi et al., 2012). The third category consists of the performed studies on presenting and modeling novel configurations with better performance. Some studies in this field were carried out by Taskar and Riggs (1997), Juarez et al. (2001), and Weifeng et al. (2007). Rahimpour (2009), proposed a novel fluidized-bed membrane reactor for naphtha reforming in the presence of catalyst deactivation to enhance hydrogen production. Also Mostafazadeh and Rahimpour (2009) assessed the membrane insertion in naphtha reforming catalytic bed

by considering catalyst deactivation. Recently, Iranshahi et al. (2010a,b,c) and Rahimpour et al. (2011) proposed new configurations including axial flow spherical reactor, axial flow spherical membrane reactor, radial flow spherical reactor, and thermally coupled fixed bed reactors for naphtha reforming process to boost hydrogen and aromatic production in refineries. As discussed in this literature survey, various studies have been done on the naphtha reforming process, but few studies have been carried out on the continuous catalyst regeneration system. Hongjun et al. (2010), Weifeng et al. (2007), and Mahdavian et al. (2010) introduced modeling and simulations approaches for CCR process.

## 2. Kinetic model

An effective kinetic model of naphtha reforming must represent all the major types of reactions in the reforming process. A kinetic model inherently satisfies both heat and material balances; because it takes into account the stoichiometry of the reactions. As discussed, the naphtha feedstock consists of several hundred components and each of them takes part in various reactions. Thus, presenting a detailed kinetics-based model considering all components and reactions is infeasible. In past decades, many attempts have been made (Marin et al., 1983; Froment, 1987; Ramage et al., 1987; Jorge and Eduardo, 2000; Hu et al., 2003; Weifeng et al., 2006) to propose a perfect kinetic model for naphtha reforming process by considering most kinetic lumps and reactions. Padmavathi and Chaudhuri (1997) proposed appropriate model for naphtha reforming kinetic, but in their model, some of the main lumps and reactions have been ignored. While in the reforming process, aromatics are the main products, 8-carbon aromatics were not subdivided in details. In addition, some of the main reactions such as dehydrocyclization of paraffins to aromatics, isomerization and transalkylation of aromatics have been ignored. In the proposed model, 8-carbon aromatics are subdivided to four lumps (ethylbenzene, para-xylene, meta-xylene and ortho-xylene) and the variations of each of them are investigated. Also ignored reactions in Padmavathi and Chaudhuri (1997) study, are characterized in Tables 1–9.

Proper kinetic modeling of reforming reactions is the key to effective representation of the process over a wide operating range. The first effect of the kinetics of the reactions on the product properties is the effect of operating variables on the octane number (Taskar and Riggs, 1997). Therefore, by considering important kinetics in the reforming process and all of the accomplished studies, in this study, a new reaction network is proposed.

Paraffins, naphthenes and aromatics are the different hydrocarbon groups in the reforming feedstock. In the presented model, the naphtha feedstock has been subdivided to naphthenes (alkylcyclohexanes: ACH, alkylcyclopentanes: ACP), paraffins (normal paraffins: NP, isoparaffins: IP), and aromatics (A) lumps with carbon numbers ranging from  $C_6$  to  $C_{9+}$ , this kinetic model consists of 32 pseudo components with 84 reactions. As shown in Fig. 2, in this model, all of the main reactions are included, and the defined pseudo components are related by major reforming reactions. In addition, rate constants in the proposed model are obtained by optimization, so that deviation between output results of model and commercial data is minimized. In the following, main reactions in the reforming process are discussed, and the reactions, rate

**Table 1 – Rate constants and heat of reactions in dehydrogenation reactions.**

(1)	$\text{ACH}_n \leftrightarrow A_n + 3\text{H}_2$	$r_{1n} = k_{1n} \left( P_{\text{ACH}_n} - \frac{P_{A_n} P_{\text{H}_2}^3}{K_{1n}} \right)$	$k_{1n} = \exp \left( a - \frac{E}{RT} \right) (\text{kmol kg}_{\text{cat}}^{-1} \text{h}^{-1} \text{kPa}^{-1})$	$K_{1n} = \exp \left( A - \frac{B}{T} \right) (\text{kPa})^3$	
C <sub>6</sub>	$\Delta H (\text{kJ molH}_2^{-1})$	$a$	$\frac{E}{R}$	A	B
C <sub>7</sub>	68.73	18.75	19.50	59.90	$24.80 \times 10^3$
C <sub>8</sub>	208.47	20.70	19.50	60.23	$25.08 \times 10^3$
for $A_n = MX^a$	64.50	17.89	19.50	60.37	$23.27 \times 10^3$
for $A_n = OX^a$	65.10	19.15	19.50	60.32	$23.49 \times 10^3$
for $A_n = PX^a$	64.74	18.66	19.50	60.13	$23.36 \times 10^3$
for $A_n = EB^a$	68.70	18.71	19.50	60.40	$24.78 \times 10^3$
C <sub>9</sub> <sup>+</sup>	66.05	20.38	19.50	61.05	$21.33 \times 10^3$

<sup>a</sup> Ignored reactions in Padmavathi and Chaudhuri (1997) study.

constants, characteristics and the calculated heat of reactions are listed.

## 2.1. Dehydrogenation

Dehydrogenation reaction, due to produce high octane number aromatics, is a principal reaction in the reforming process (Matar and Hatch, 2000). Octane number is gained at a loss of volume, when a naphthalene is converted to an aromatic (Taskar and Riggs, 1997). This reaction is the fastest amongst all the reforming reactions, thus reaches equilibrium very quickly and is catalyzed by the metallic function of the

catalyst (Antos and Aitani, 1995; Taskar and Riggs, 1997). The reaction is endothermic and produces a sharp drop in temperature. The needed reaction constants for calculating the reaction rate constants ( $k_{1n}$ ) and equilibrium constants ( $K_{1n}$ ) are presented in Table 1.

## 2.2. Dehydrocyclization

Dehydrocyclization of paraffins to naphthenes and aromatics is a desirable reaction in the reforming process because it induces the most considerable increase in octane number among the naphtha reforming reactions. But unfortunately,

**Table 2 – Rate constants and heat of reaction in paraffin dehydrocyclization to naphthene.**

(2)	$\text{ACH}_n + \text{H}_2 \leftrightarrow \text{NP}_n$	$r_{2n} = k_{2n} \left( P_{\text{ACH}_n} P_{\text{H}_2} - \frac{P_{\text{NP}_n}}{K_{2n}} \right)$	$k_{2n} = \exp \left( a - \frac{E}{RT} \right) (\text{kmol kg}_{\text{cat}}^{-1} \text{h}^{-1} \text{kPa}^{-2})$	$K_{2n} = \exp \left( A - \frac{B}{T} \right) (\text{kPa})^{-1}$	
C <sub>6</sub>	$\Delta H (\text{kJ mol}^{-1})$	$a$	$\frac{E}{R}$	A	B
C <sub>6</sub>	-43.64	24.37	33.11	-9.12	$-5.24 \times 10^3$
C <sub>7</sub>	-32.85	29.10	33.11	-8.95	$-3.95 \times 10^3$
C <sub>8</sub>	-32.55	27.81	33.11	-8.34	$-3.91 \times 10^3$
C <sub>9</sub> <sup>+</sup>	-28.00	29.76	33.11	-8.12	$-3.37 \times 10^3$
(3)	$\text{ACH}_n + \text{H}_2 \leftrightarrow \text{IP}_n$	$r_{3n} = k_{3n} \left( P_{\text{ACH}_n} P_{\text{H}_2} - \frac{P_{\text{IP}_n}}{K_{3n}} \right)$	$k_{3n} = \exp \left( a - \frac{E}{RT} \right) (\text{kmol kg}_{\text{cat}}^{-1} \text{h}^{-1} \text{kPa}^{-2})$	$K_{3n} = \exp \left( A - \frac{B}{T} \right) (\text{kPa})^{-1}$	
C <sub>6</sub>	$\Delta H (\text{kJ mol}^{-1})$	$a$	$\frac{E}{R}$	A	B
C <sub>6</sub>	-52.00	26.36	33.11	-14.35	$-6.25 \times 10^3$
C <sub>7</sub>	-39.30	25.75	33.11	-13.65	$-4.73 \times 10^3$
C <sub>8</sub>	-49.40	29.00	33.11	-13.17	$-5.94 \times 10^3$
C <sub>9</sub> <sup>+</sup>	-49.00	29.76	33.11	-12.39	$-5.89 \times 10^3$
(4)	$\text{NP}_n \leftrightarrow \text{ACP}_n + \text{H}_2$	$r_{4n} = k_{4n} \left( P_{\text{NP}_n} - \frac{P_{\text{ACP}_n} P_{\text{H}_2}}{K_{4n}} \right)$	$k_{4n} = \exp \left( a - \frac{E}{RT} \right) (\text{kmol kg}_{\text{cat}}^{-1} \text{h}^{-1} \text{kPa}^{-1})$	$K_{4n} = \exp \left( A - \frac{B}{T} \right) (\text{kPa})$	
C <sub>5</sub> <sup>a</sup>	$\Delta H (\text{kJ mol}^{-1})$	$a$	$\frac{E}{R}$	A	B
C <sub>5</sub> <sup>a</sup>	69.73	30.75	33.11	14.39	$8.38 \times 10^3$
C <sub>6</sub>	60.74	31.94	33.11	14.77	$7.31 \times 10^3$
C <sub>7</sub>	60.75	33.43	33.11	14.63	$7.31 \times 10^3$
C <sub>8</sub>	61.75	31.31	33.11	15.98	$7.43 \times 10^3$
C <sub>9</sub> <sup>+</sup>	59.00	32.96	33.11	15.21	$7.09 \times 10^3$
(5)	$\text{IP}_n \leftrightarrow \text{ACP}_n + \text{H}_2$	$r_{5n} = k_{5n} \left( P_{\text{IP}_n} - \frac{P_{\text{ACP}_n} P_{\text{H}_2}}{K_{5n}} \right)$	$k_{5n} = \exp \left( a - \frac{E}{RT} \right) (\text{kmol kg}_{\text{cat}}^{-1} \text{h}^{-1} \text{kPa}^{-1})$	$K_{5n} = \exp \left( A - \frac{B}{T} \right) (\text{kPa})$	
C <sub>5</sub> <sup>a</sup>	$\Delta H (\text{kJ mol}^{-1})$	$a$	$\frac{E}{R}$	A	B
C <sub>5</sub> <sup>a</sup>	76.67	29.83	33.11	16.18	$9.22 \times 10^3$
C <sub>6</sub>	70.60	30.87	33.11	16.03	$8.50 \times 10^3$
C <sub>7</sub>	67.20	32.95	33.11	15.47	$8.08 \times 10^3$
C <sub>8</sub>	78.60	34.19	33.11	16.37	$9.45 \times 10^3$
C <sub>9</sub> <sup>+</sup>	80.00	32.96	33.11	16.02	$9.62 \times 10^3$

<sup>a</sup> Ignored reactions in Padmavathi and Chaudhuri (1997) study.

**Table 3 – Rate constants and heat of reactions in paraffin dehydrocyclization to aromatic.**

(6) $\text{NP}_n \leftrightarrow \text{A}_n + 4\text{H}_2$ $r_{6n} = k_{6n}(P_{\text{NP}_n} - \frac{P_{\text{A}_n} P_{\text{H}_2}^4}{K_{6n}})$ $k_{6n} = \exp(a - \frac{E}{RT})$ (kmol kg <sub>cat</sub> <sup>-1</sup> h <sup>-1</sup> kPa <sup>-1</sup> ) $K_{6n} = \exp(A - \frac{B}{T})$ (kPa) <sup>4</sup>					
	$\Delta H(\text{kJ}(\text{mol H}_2)^{-1})$	$a$	$\frac{E}{R}$	A	B
C <sub>6</sub> <sup>a</sup>	66.50	16.87	18.86	35.73	$7.99 \times 10^3$
C <sub>7</sub> <sup>a</sup>	63.20	17.17	18.86	35.21	$7.60 \times 10^3$
C <sub>8</sub> <sup>a</sup>					
for A <sub>n</sub> = MX	56.51	17.32	18.86	34.13	$6.79 \times 10^3$
for A <sub>n</sub> = OX	56.95	17.89	18.86	34.21	$6.85 \times 10^3$
for A <sub>n</sub> = PX	56.70	17.01	18.86	34.16	$6.81 \times 10^3$
for A <sub>n</sub> = EB	59.66	16.96	18.86	34.63	$7.17 \times 10^3$
C <sub>9+</sub> <sup>a</sup>	59.29	18.90	18.86	33.56	$6.36 \times 10^3$
(7) $\text{IP}_n \leftrightarrow \text{A}_n + 4\text{H}_2$ $r_{7n} = k_{7n}(P_{\text{IP}_n} - \frac{P_{\text{A}_n} P_{\text{H}_2}^4}{K_{7n}})$ $k_{7n} = \exp(a - \frac{E}{RT})$ (kmol kg <sub>cat</sub> <sup>-1</sup> h <sup>-1</sup> kPa <sup>-1</sup> ) $K_{7n} = \exp(A - \frac{B}{T})$ (kPa) <sup>4</sup>					
	$\Delta H(\text{kJ}(\text{mol H}_2)^{-1})$	$a$	$\frac{E}{R}$	A	B
C <sub>6</sub> <sup>a</sup>	68.18	16.44	18.86	36.01	$8.20 \times 10^3$
C <sub>7</sub> <sup>a</sup>	64.83	16.90	18.86	35.47	$7.79 \times 10^3$
C <sub>8</sub> <sup>a</sup>					
for A <sub>n</sub> = MX	60.73	16.27	18.86	34.81	$7.30 \times 10^3$
for A <sub>n</sub> = OX	61.17	16.78	18.86	34.87	$7.35 \times 10^3$
for A <sub>n</sub> = PX	60.90	16.04	18.86	34.83	$7.32 \times 10^3$
for A <sub>n</sub> = EB	63.88	15.93	18.86	35.23	$7.68 \times 10^3$
C <sub>9+</sub> <sup>a</sup>	60.77	17.66	18.86	34.81	$7.3 \times 10^3$

<sup>a</sup> Ignored reactions in Padmavathi and Chaudhuri (1997) study.

**Table 4 – Rate constants and heat of reactions in isomerization of naphthenes and paraffins.**

(8) $\text{ACP}_n \leftrightarrow \text{ACH}_n$ $r_{8n} = k_{8n}(P_{\text{ACP}_n} - \frac{P_{\text{ACH}_n}}{K_{8n}})$ $k_{8n} = \exp(a - \frac{E}{RT})$ (kmol kg <sub>cat</sub> <sup>-1</sup> h <sup>-1</sup> kPa <sup>-1</sup> ) $K_{8n} = \exp(A - \frac{B}{T})$ (-)					
	$\Delta H(\text{kJ mol}^{-1})$	$a$	$\frac{E}{R}$	A	B
C <sub>6</sub>	-17.10	15.11	23.81	-5.20	$-2.06 \times 10^3$
C <sub>7</sub>	-27.90	24.73	23.81	-6.63	$-3.36 \times 10^3$
C <sub>8</sub>	-29.20	25.78	23.81	-6.83	$-3.51 \times 10^3$
C <sub>9+</sub>	-31.00	26.13	23.81	-7.16	$-3.73 \times 10^3$
(9) $\text{NP}_n \leftrightarrow \text{IP}_n$ $r_{9n} = k_{9n}(P_{\text{NP}_n} - \frac{P_{\text{IP}_n}}{K_{9n}})$ $k_{9n} = \exp(a - \frac{E}{RT})$ (kmol kg <sub>cat</sub> <sup>-1</sup> h <sup>-1</sup> kPa <sup>-1</sup> ) $K_{9n} = \exp(A - \frac{B}{T})$ (-)					
	$\Delta H(\text{kJ mol}^{-1})$	$a$	$\frac{E}{R}$	A	B
C <sub>4</sub> <sup>a</sup>	-9.23	25.08	26	0.80	$-1.11 \times 10^3$
C <sub>5</sub> <sup>a</sup>	-6.94	24.89	26	1.17	$-0.83 \times 10^3$
C <sub>6</sub>	-9.86	24.70	26	0.69	$-1.19 \times 10^3$
C <sub>7</sub>	-6.45	24.15	26	1.27	$-0.76 \times 10^3$
C <sub>8</sub>	-13.95	25.54	26	0.04	$-1.68 \times 10^3$
C <sub>9+</sub>	-21.00	24.48	26	-1.09	$-2.53 \times 10^3$

<sup>a</sup> Ignored reactions in Padmavathi and Chaudhuri (1997) study.

**Table 5 – Rate constants and heat of reactions in isomerization of aromatics.**

(10) $\text{R} \leftrightarrow \text{P}$ for $n = 1, \dots, 6$ $r_{10n} = k_{10n}(P_{\text{R}} - \frac{P_{\text{P}}}{K_{10n}})$ $k_{10n} = \exp(a - \frac{E}{RT})$ (kmol kg <sub>cat</sub> <sup>-1</sup> h <sup>-1</sup> kPa <sup>-1</sup> ) $K_{10n} = \exp(A - \frac{B}{T})$ (-)					
R	P	$\Delta H(\text{kJ mol}^{-1})$	$a$	$\frac{E}{R}$	A
n = 1 <sup>a</sup>	OX	PX	-10.50	25.21	21.24
n = 2 <sup>a</sup>	OX	MX	-17.60	24.50	21.24
n = 3 <sup>a</sup>	MX	EB	12.60	24.53	21.24
n = 4 <sup>a</sup>	OX	EB	10.84	25.17	21.24
n = 5 <sup>a</sup>	EB	PX	-11.89	25.84	21.24
n = 6 <sup>a</sup>	MX	PX	0.71	24.47	21.24
					B
					$-1.26 \times 10^3$
					$-2.11 \times 10^3$
					$1.50 \times 10^3$
					$1.30 \times 10^3$
					$-1.43 \times 10^3$
					$-0.085 \times 10^3$

<sup>a</sup> Ignored reactions in Padmavathi and Chaudhuri (1997) study.

**Table 6 – Rate constants and heat of reactions in Transalkylation.**

$$(11) 2R \leftrightarrow P + C \text{ for } n = 7, 8 \quad r_{11n} = k_{11n} \left( P_R^2 - \frac{P_P P_C}{K_{11n}} \right) \quad k_{11n} = \exp \left( a - \frac{E}{RT} \right) \quad (\text{kmol kg}_{\text{cat}}^{-1} \text{ h}^{-1} \text{ kPa}^{-2}) \quad K_{11n} = \exp \left( A - \frac{B}{T} \right) \quad (-)$$

R	P	C	$\Delta H \text{ (kJ mol}^{-1}\text{)}$	a	$\frac{E}{R}$	A	B
$n=7^{\text{a}}$	T	B	PX	16.20	16.68	21.24	16.41
$n=8^{\text{a}}$	OX	T	$A_{9+}$	09.16	15.48	21.24	15.28

<sup>a</sup> Ignored reactions in Padmavathi and Chaudhuri (1997) study.

these reactions are the most difficult reaction to promote (Matar and Hatch, 2000). The most reactions of dehydrocyclization are endothermic and promoted by high temperature, low pressure and by both metallic and acidic functions of the catalyst. The needed reaction constants for calculating the reaction rate constants ( $k_{2n}$ ,  $k_{3n}$ ,  $k_{4n}$ ,  $k_{5n}$ ,  $k_{6n}$  and  $k_{7n}$ ) and equilibrium constants ( $K_{2n}$ ,  $K_{3n}$ ,  $K_{4n}$ ,  $K_{5n}$ ,  $K_{6n}$  and  $K_{7n}$ ) of dehydrocyclization reactions are presented in Tables 2 and 3.

### 2.3. Isomerization

Three types of isomerization reactions are investigated in the reforming process, including isomerization of paraffins, naphthenes and aromatics. Paraffins isomerization rearranges the molecule with essentially no change in the volume. These reactions are fast, slightly exothermic and do not affect

the number of carbon atoms (Matar and Hatch, 2000). The reactions are unaffected by pressure, while from a kinetic viewpoint, the equilibrium depends mainly on the temperature. It should be mentioned that isomerization reactions are promoted by the acidic function (Antos and Aitani, 1995). The isomerization of alkylcyclopentanes into alkylcyclohexanes involves a ring rearrangement. In the subsequent stage, the produced alkylcyclohexanes undergo dehydrogenation reaction and produce aromatics. Thus, isomerization of naphthenes is considered as a desirable reaction. Aromatics with 8-carbon atoms also undergo the isomerization reactions, the isomerization between P-xylene, M-xylene and O-xylene occur rapidly, while isomerization between ethylbenzene and xylene isomer occurs slowly (Weifeng et al., 2006). Calculated constants for isomerization reactions of naphthenes, paraffins and aromatics are shown in Tables 4 and 5.

**Table 7 – Rate constants and heat of reactions in Cracking of Paraffins.**

for $n = 2$	for $n = 3$		
$P_2 + H_2 \rightarrow 2P_1$	$P_3 + H_2 \rightarrow P_1 + P_2$		
for $n = 4$	for $n = 5$		
(12) $NP_4 + H_2 \rightarrow \frac{2}{3}(P_3 + P_2 + P_1)$	$NP_5 + H_2 \rightarrow \frac{1}{2}(NP_4 + P_3 + P_2 + P_1)$		
for $n = 6 - 9$ :			
$NP_n + \frac{n-3}{3}H_2 \rightarrow \frac{n}{15} \sum_{i=1}^5 P_i$	$r_{12n} = k_{12n} \left( \frac{P_{NP_n}}{P_t} \right)$		
	$k_{12n} = \exp \left( a - \frac{E}{RT} \right) \quad (\text{kmol kg}_{\text{cat}}^{-1} \text{ h}^{-1})$		
	$\Delta H(\text{kJ (mol H}_2)^{-1}\text{)}$		
	a		
	$\frac{E}{R}$		
$C_2^{\text{a}}$	-65.20	37.85	34.61
$C_3^{\text{a}}$	-53.60	39.95	34.61
$C_4^{\text{a}}$	-49.50	40.15	34.61
$C_5^{\text{a}}$	-47.80	41.60	34.61
$C_6$	-47.26	42.08	34.61
$C_7$	-46.69	42.48	34.61
$C_8$	-46.61	40.53	34.61
$C_{9+}$	-46.15	43.85	34.61
for $n = 4$ $IP_4 + \frac{3}{2}H_2 \rightarrow \frac{1}{2}(3P_1 + P_2 + P_3)$	for $n = 6 - 9$ :		
(13) for $n = 5$ $IP_5 + H_2 \rightarrow \frac{1}{2}(IP_4 + P_3 + P_2 + P_1)$	$IP_n + \frac{n-3}{3}H_2 \rightarrow \frac{n}{15} \sum_{i=1}^5 P_i$		
$r_{13n} = k_{13n} \left( \frac{P_{IP_n}}{P_t} \right)$	$k_{13n} = \exp \left( a - \frac{E}{RT} \right) \quad (\text{kmol kg}_{\text{cat}}^{-1} \text{ h}^{-1})$		
	$\Delta H(\text{kJ (mol H}_2)^{-1}\text{)}$		
	a		
	$\frac{E}{R}$		
$C_4^{\text{a}}$	-40.30	36.15	34.61
$C_5^{\text{a}}$	-45.30	41.57	34.61
$C_6$	-37.40	40.53	34.61
$C_7$	-41.85	41.57	34.61
$C_8$	-36.00	41.51	34.61
$C_{9+}$	-35.65	42.93	34.61

<sup>a</sup> Ignored reactions in Padmavathi and Chaudhuri (1997) study.

**Table 8 – Rate constants and heat of reactions in cracking of naphthalenes.**

(14) $\text{ACH}_n + \frac{n}{3}\text{H}_2 \rightarrow \frac{n}{15} \sum_{i=1}^5 P_i \quad r_{14n} = k_{14n} \left( \frac{P_{\text{ACH}_n}}{P_t} \right) \quad k_{14n} = \exp \left( a - \frac{E}{RT} \right) (\text{kmol kg}_{\text{cat}}^{-1} \text{h}^{-1})$					
	$\Delta H(\text{kJ}(\text{mol H}_2)^{-1})$	$a$		$\frac{E}{R}$	
C <sub>6</sub>	-45.45	42.15		34.61	
C <sub>7</sub>	-40.76	44.70		34.61	
C <sub>8</sub>	-41.00	43.90		34.61	
C <sub>9+</sub>	-40.10	44.15		34.61	
for $n = 5$ : $r_{15n} = k_{15n} \left( \frac{P_{\text{ACP}_n}}{P_t} \right)$					
(15) for $n = 6 - 9$ : $\text{ACP}_n + 2\text{H}_2 \rightarrow \frac{1}{2}(\text{NP}_4 + \text{P}_3 + \text{P}_2 + \text{P}_1) \quad k_{15n} = \exp \left( a - \frac{E}{RT} \right) (\text{kmol kg}_{\text{cat}}^{-1} \text{h}^{-1})$					
	$\Delta H(\text{kJ}(\text{mol H}_2)^{-1})$	$a$		$\frac{E}{R}$	
C <sub>5</sub> <sup>a</sup>	-68.74	40.23		34.61	
C <sub>6</sub>	-54.00	41.55		34.61	
C <sub>7</sub>	-52.71	43.75		34.61	
C <sub>8</sub>	-51.95	43.65		34.61	
C <sub>9+</sub>	-50.40	44.15		34.61	

<sup>a</sup> Ignored reactions in Padmavathi and Chaudhuri (1997) study.

## 2.4. Transalkylation

Transalkylation is the reaction between two similar or dissimilar molecules involving transfer of an alkyl group. In the alkyl-transfer reactions, shift of alkyl groups from one ring to the other, depends on the number of alkyl groups on the aromatic ring/s, the type of alkyl substituent/s and the chain length (Roldán et al., 2004). In the proposed model, transalkylation between aromatics is considered. Two toluene rings can disproportionate to produce one benzene ring and one Para xylene ring, in addition, two Ortho-xylene rings disproportionate to produce one toluene and higher aromatics (A<sub>9+</sub>). These reactions are promoted by the catalyst metallic function, and with increase in the reaction temperature, the conversion increases. It should be mentioned that transalkylation occurs mainly in very severe conditions of pressure (Roldán et al., 2004). Calculated constants for reaction rate in the transalkylation reactions are presented in Table 6.

## 2.5. Hydrocracking

Breaking of carbon bonds in the reforming is called hydrocracking. Bond's breaking can occur at any position along the hydrocarbon chain. This reaction by removing the low octane number paraffins and naphthalenes from reformate and producing lighter hydrocarbons, such as methane, ethane and propane, helps to improve the octane in the products (Matar and Hatch, 2000). Hydrocracking is an irreversible reaction and is favored at high temperature and high pressure, also is catalyzed by the acidic or metallic function of the catalyst (Antos and Aitani, 1995; Matar and Hatch, 2000). Reaction constants for hydrocracking of paraffins and naphthalenes are shown in Tables 7 and 8, respectively.

## 2.6. Hydrodealkylation

Hydrodealkylation is the breakage (or cleavage) of the branched radical of aromatics ring in presence of

**Table 9 – Rate constants and heat of reactions in hydrodealkylations.**

(16) $\text{A}_{n+1} + \text{H}_2 \rightarrow \text{A}_k + \text{C}_m\text{H}_{2m+2} \quad r_{16n} = k_{16n} P_{\text{A}_{n+1}} P_{\text{H}_2}^{0.5} \quad k_{16n} = \exp \left( a - \frac{E}{RT} \right) (\text{kmol kg}_{\text{cat}}^{-1} \text{h}^{-1} \text{kPa}^{-1.5})$					
	$m$	$k$	$\Delta H(\text{kJ}(\text{mol H}_2)^{-1})$	$a$	$\frac{E}{R}$
C <sub>7</sub>	1	$n$	-41.81	7.64	17.92
C <sub>8</sub>					
for $\text{A}_{n+1} = \text{PX}$	1	$n$	-42.32	5.57	17.92
for $\text{A}_{n+1} = \text{EB}^a$	2	$n - 1$	-20.02	5.55	17.92
C <sub>9+</sub>					
for $\text{A}_k = \text{OX}$	1	$n$	-52.57	8.91	17.92
for $\text{A}_k = \text{T}^a$	2	$n - 1$	-30.80	5.57	17.92

<sup>a</sup> Ignored reactions in Padmavathi and Chaudhuri (1997) study.

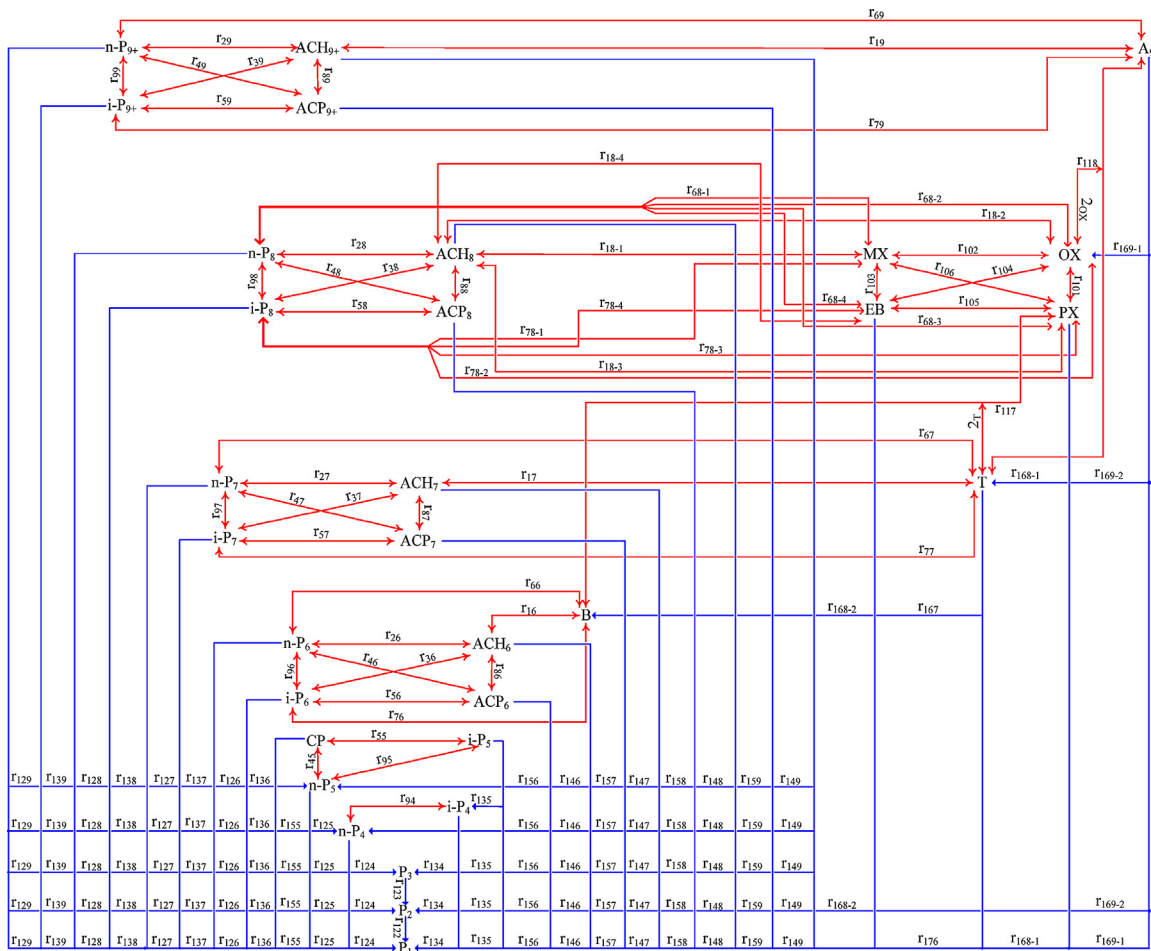


**Fig. 2 – Reaction network scheme for naphtha reforming process.**

hydrogen. Like hydrocracking, this reaction is favored by high temperature and high pressure also it is an irreversible reaction, and promoted by the metallic function of the catalyst. hydrodealkylation is the slowest of all the reforming reactions. This reaction is desirable because it changes the relative equilibrium distribution of the aromatics in favor of benzene and octane number (Taskar and Riggs, 1997; Matar and Hatch, 2000). The needed hydrodealkylation constants to calculate the reaction rate constants ( $k_{16n}$ ) is presented in Table 9.

### 3. Process description

The Continuous Catalyst Regeneration (CCR) process is a part of process used in the petroleum and petrochemical industries. With the advent of the continuous catalytic regeneration process, significant progress was observed. Also, catalytic reformers and in particular, continuous catalyst regeneration, have indispensable role in the refiners' plans due to current environment regulations for reducing air pollutants induced by sulfur of gasoline (Aitani, 2005a,b).

The CCR process consists of regeneration unit and adiabatic cross-flow reactors that are arranged in a conventional side-by-side pattern. As shown in Fig. 3, the first reactor is always smaller than the other reactors and the last reactor is always the largest. In this process, each catalyst particle moves continuously from the first reactor toward the last reactor. Then, catalyst particles are sent to the regeneration unit to restore. Also, hydrotreated naphtha is combined with the

recycle hydrogen gas and, after heating to the desired reaction temperature (798 K), it is sent to a series of reactors. The specification of conventional process such as reactors, feed, product and catalyst are shown in Table 10.

In the CCR process, spherical catalysts are used in the reactors to facilitate catalyst circulation by gravity. Coked catalyst is withdrawn from the last reactor and sent to the regeneration unit, then, regeneration of the catalyst is performed as the catalyst moves down in the regeneration unit on a continuous basis. Regenerated catalyst is added to the top of the first reactor to keep the efficiency of process at the certain level, and catalyst regeneration leads to reduction in operating cost, whiles, poor catalyst will lead to low product yields and increase in operating expense. As shown in Fig. 4, catalyst flows vertically in the reactor; and the feed flows radially through the catalyst bed (reaction side) of the reactor, thus cross flow pattern exist in the reactors.

### 4. Catalyst deactivation model

Coke deposition on the catalyst is an undesirable by-product in the reforming process, and the amount of deposited coke depends on feed quality, catalyst state and transit time of catalyst from the reactors (Taskar and Riggs, 1997). Catalyst deactivation is primarily a function of coke deposition on the catalyst. Controlling coke deposition is equivalent to controlling catalyst deactivation. In the CCR process, the catalyst circulation rate can be adjusted to maintain a specified weight percent carbon on the catalyst (Antos and Aitani, 1995).

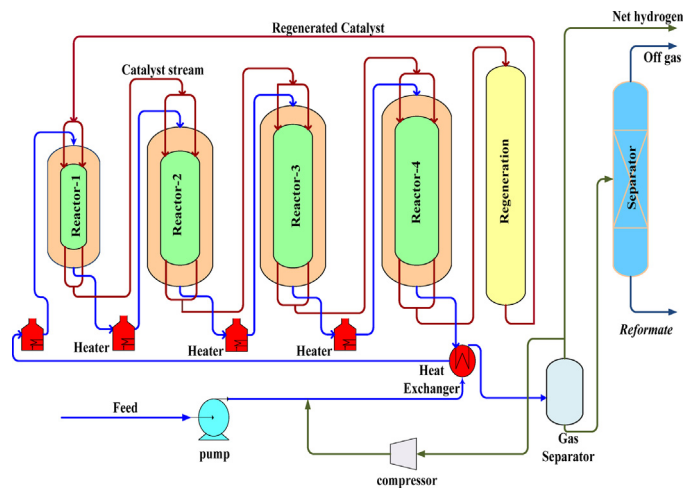


**Fig. 3 – Process flow scheme for CCR reforming process.**

The main characteristics of a catalyst are: activity, selectivity and stability (Barbier, 1986). The activity expresses the catalyst ability to increase the rate of the reactions. The selectivity expresses the catalyst ability to favor desirable reactions rather than others. The stability characterizes the change of the catalyst performance with time (i.e. activity and selectivity) while operating conditions and feed are stable. The catalyst affects reaction rates through its two different functions: metallic and acidic, which promote different type of reactions (Carter et al., 1982). Coking on the metallic and acidic

functions directly affect the selectivity of reactions (Lieske et al., 1987). Catalysts used in this processes are bimetallic Pt-Sn and support is high purity alumina (acidic function). The metal site is provided by platinum and metal promoter is tin. The reaction in this process starts on the metal sites and continues on the acid sites (Carter et al., 1982; Lieske et al., 1987).

The metallic function is mainly responsible for dehydrogenation, transalkylation and hydrodealkylation activity and these reactions are practically unaffected by the presence or

**Table 10 – Specifications of reactors, feed, product and catalyst of plant for fresh catalyst.**

Parameter	Numerical value				Unit
	1st reactor	2nd reactor	3rd reactor	4th reactor	
Naphtha feed stock	233637.01				kg/h
Reformatte	216488.63				kg/h
H <sub>2</sub> /HC mole ratio	2.193				—
Mole percent of hydrogen in recycle	0.83				—
Inlet temperature (K)	798	798	798	798	798
Inlet pressure (kPa)	595	550	505	460	460
Inner and outer Diameter (m)	1.25, 2.19	1.25, 2.35	1.30, 2.53	1.3, 2.89	1.3, 2.89
Length (m)	8.50	10.35	12.1	15.39	15.39
Catalyst distribution (wt %)	12	18	25	45	45
<b>Distillation fraction of naphtha feed</b>					
ASTM D86	Naphtha feed (°C)				
IBP	81				
5%	91.2				
10%	93.2				
20%	96.9				
30%	101.1				
40%	105.7				
50%	111.4				
60%	117.6				
70%	124.5				
80%	132.7				
90%	143.1				
95%	150.5				
FBP	159				
<b>Typical properties of catalyst</b>					
d <sub>p</sub>	1.8				mm
Pt	0.3				wt%
Sn	0.3				wt%
S <sub>a</sub>	220				m <sup>2</sup> /g
ρ <sub>B</sub>	680				kg/m <sup>3</sup>
ε	0.36				—

**Table 11 – Catalyst functions on the main reactions in the proposed kinetic model (metallic (M) and acidic (A) functions).**

Reactions		Agent	Reactions		Agent
$r_{1n}$	$\text{ACH}_n \leftrightarrow \text{A}_n + 3\text{H}_2$	M	$r_{9n}$	$\text{NP}_n \leftrightarrow \text{IP}_n$	A
$r_{2n}$	$\text{ACH}_n + \text{H}_2 \leftrightarrow \text{NP}_n$	M + A	$r_{10n}$	$\text{R} \leftrightarrow \text{P}$	A
$r_{3n}$	$\text{ACH}_n + \text{H}_2 \leftrightarrow \text{IP}_n$	M + A	$r_{11n}$	$2\text{R} \leftrightarrow \text{P} + \text{C}$	M
$r_{4n}$	$\text{NP}_n \leftrightarrow \text{ACP}_n + \text{H}_2$	M + A	$r_{12n}$	$\text{NP}_n + \frac{(n-3)}{3}\text{H}_2 \rightarrow \frac{n}{15} \sum_{i=1}^5 \text{P}_i$	M or A
$r_{5n}$	$\text{IP}_n \leftrightarrow \text{ACP}_n + \text{H}_2$	M + A	$r_{13n}$	$\text{IP}_n + \frac{(n-3)}{3}\text{H}_2 \rightarrow \frac{n}{15} \sum_{i=1}^5 \text{P}_i$	M or A
$r_{6n}$	$\text{NP}_n \rightarrow \text{A}_n + 4\text{H}_2$	M + A	$r_{14n}$	$\text{ACH}_n + \frac{n}{3}\text{H}_2 \rightarrow \frac{n}{15} \sum_{i=1}^5 \text{P}_i$	M or A
$r_{7n}$	$\text{IP}_n \leftrightarrow \text{A}_n + 4\text{H}_2$	M + A	$r_{15n}$	$\text{ACP}_n + \frac{n}{3}\text{H}_2 \rightarrow \frac{n}{15} \sum_{i=1}^5 \text{P}_i$	M or A
$r_{8n}$	$\text{ACP}_n \leftrightarrow \text{ACH}_n$	A	$r_{16n}$	$\text{A}_{n+1} + \text{H}_2 \rightarrow \text{A}_k + \text{C}_m\text{H}_{2m+2}$	M

absence of acid sites, while the acidic support provides activity for the isomerization reactions. Two of the naphtha reforming reactions (hydrocracking and dehydrocyclization) can also be catalyzed by the metallic and acidic function (Antos and Aitani, 1995; Barbier, 1986; Lieske et al., 1987). Table 11 shows the catalyst functions on the main reactions in the proposed kinetic model.

This section proposes a model for catalyst deactivation rate that is developed on the basis of pilot-plant data

and published literatures. According to previous studies (Figoli et al., 1983a,b; Mieville, 1991; Bishara et al., 1984), the rate of deactivation depends on operating conditions such as: temperature, pressure and hydrogen over hydrocarbon mole ratio, also according to models proposed by Liu et al. (1997, 2002) and Tailleur and Davila (2008) the rate of deactivation depends on alkylcyclopentane concentrations. Thus, the rate of coke formation on the fresh catalyst could be written as follows:

$$r_C^0 \propto \frac{\exp(-E_c/RT)}{P^{n_1}(H_2/HC)^{n_2}} \times C_{ACP}^{0.5} \quad (17)$$

where  $r_C^0$ ,  $E_c$ ,  $C_{ACP}$ ,  $P$  and  $(H_2/HC)$  are the rate of coke formation on the fresh catalyst, coke formation activation energy, alkylcyclopentane concentration, pressure and hydrogen over hydrocarbon mole ratio, respectively. In addition, the rate of reaction over a spent catalyst is calculated by multiplying the catalyst activity on the dominant function and rate of reaction over fresh catalyst.

$$r_i = a_i \times r_i^0 \quad (18)$$

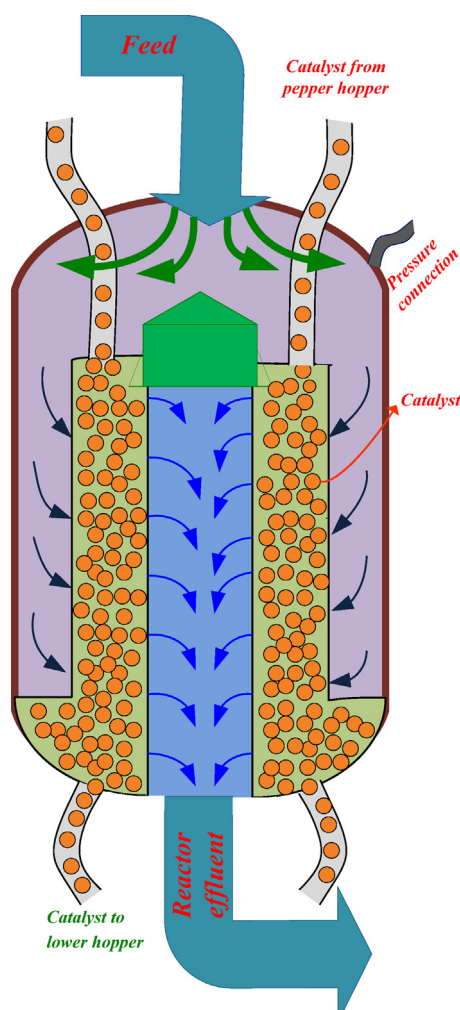
where  $r_i$  represents the  $i$ th reaction. The catalyst activity ( $a_i$ ) is a function of deposited coke weight fraction, which could be written as:

$$-\frac{da_i}{dC_{C_i}} = \alpha_i \times a_i^{n_i} \begin{cases} \text{If } n_i = 1 \quad a_i = \exp(-\alpha_i \times C_{C_i}) \\ \text{If } n_i \neq 1 \quad a_i = \frac{1}{(1 + (n_i - 1)\alpha_i \times C_{C_i})^{(1/(n_i - 1))}} \end{cases} \quad (19)$$

In the recent equation,  $\alpha_i$  is a constant and  $n_i$  is a power number of dominant function activity. Also,  $C_{C_i}$  is the coke weight fraction on the dominant function, that, to calculate  $C_{C_i}$ , coke formation rate must be considered, as:

$$r_{C_i} = a_{C_i} \times r_{C_i}^0, \quad (20)$$

where  $r_{C_i}$  and  $r_{C_i}^0$  are coke formation rate of spent catalyst on dominant function and rate of coke formation on dominant function of fresh catalyst, respectively. Similar to catalyst activity in the reaction rate, catalyst activity in coke formation

**Fig. 4 – Structure of reforming reactor in CCR process.**

rate also is a function of deposited coke weight fraction, which could be defined as:

$$-\frac{da_{C_i}}{dC_{C_i}} = \alpha_{C_i} \times a_{C_i}^{n_{C_i}} \begin{cases} \text{If } n_{C_i} = 1 \quad a_{C_i} = \exp(-\alpha_{C_i} \times C_{C_i}) \\ \text{If } n_{C_i} \neq 1 \quad a_i = \frac{1}{(1 + (n_{C_i} - 1)\alpha_{C_i} \times C_{C_i})^{1/(n_{C_i}-1)}} \end{cases} \quad (21)$$

In the recent equation,  $a_{C_i}$  is activity of dominant function for coke formation,  $n_{C_i}$  is activity power number, and  $\alpha_{C_i}$  is a constant. As previously discussed, reaction rate is affected by catalyst functions (metallic and acidic). If the reaction occurs on the metallic site of catalyst, metallic function activity must be considered i.e.  $a_i = a_M$ . In other case, when reaction occurs on catalyst acidic site, acidic function activity must be considered i.e.  $a_i = a_A$ . Finally, if one of the catalyst functions is needed (acidic or metallic), or both functions of the catalyst are required, the mean activities must be considered. The obtained relations for calculating catalyst deactivation rate based on catalyst functions in the reforming reaction are presented in Table 12. The auxiliary correlations are described in Appendix A.

## 5. Mathematical modeling

To develop a model for CCR process, heat and material balance equations are made over a small element of the reactor with the length of  $\Delta z$  and the thickness of  $\Delta r$ . Then these equations are combined with the deactivation model, Ergun equation, also thermodynamic and kinetic relations as auxiliary correlations for predicting the behavior of reforming process. In the previous studies, that have been done for modeling of CCR process (Hongjun et al., 2010; Weifeng et al., 2007; Mahdavian et al., 2010), variations of parameters are assumed in one dimension. While, in this study, the mathematical modeling of the reactor is done in two dimensions (radial and axial), and its results had better compliance with the actual data. A differential volume element of the reactor on which the energy and mass balance equations has been applied, is shown in Fig. 5a, also top view of this control volume is shown in Fig. 5b. The obtained results of the mathematical model are described in Table 13. Also, details of the mathematical modeling for this process are described in Appendixes B–D. Basic assumptions

To develop mathematical modeling based on mass and energy balances and other auxiliary correlations, the following assumptions are applied:

- Steady state condition is considered.
- Diffusion of mass and heat in both radial and axial directions of reactor is neglected.
- Homogeneous catalyst moving bed is considered.
- Ideal gas law is applicable. (Due to high temperature)
- Adiabatic conditions exist. (insulated outlet wall)
- Cross flow pattern is considered in the reactors. (Gas stream moves radially and catalyst moves axially downward)
- Peripheral gradient (gradient along the perimeter) is neglected.
- Physical properties are assumed to be variable during the process.
- Intra-pellet heat and mass diffusion in catalyst pellet are ignored.

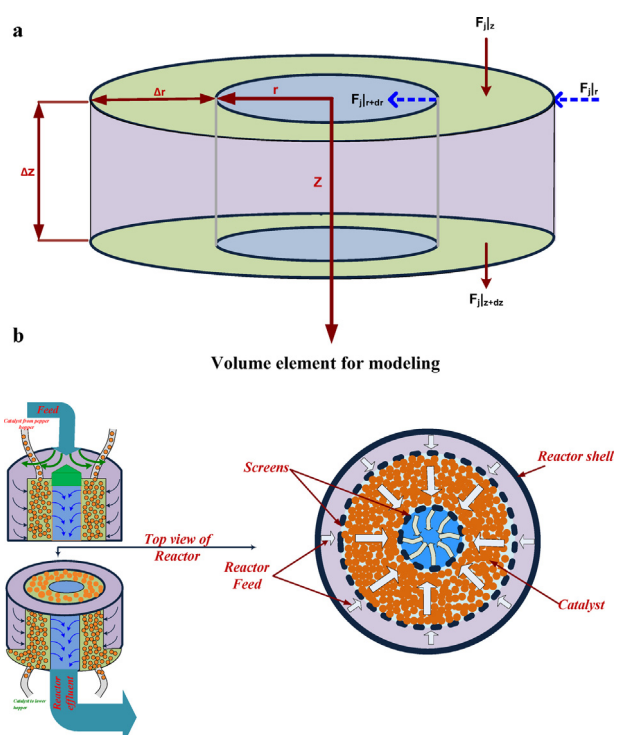


Fig. 5 – (a) Control volume for modeling with the length of  $\Delta z$  (b) top view of control volume.

## 6. Numerical solution

The obtained mathematical model in the previous section is a set of partial differential equations (PDEs). These equations are integrated through each reactor to describe the molar flow rate of reformatte and physical properties along the length and radius of the reactors. By considering these complex equations, a numerical method must be employed. In this study, finite difference method with explicit solution of all the differential equations in the mathematical model is employed. In this method, the reactor is divided into a series of nodes and for each node derivatives in differential equations become difference equations that are functions of the surrounding cells (Nauman, 2001). Then, boundary conditions of the process are used for initial nodes of the reactor and the result of each node is used as boundary conditions for the following nodes and this procedure is repeated for all nodes in the reactor (Nauman, 2001).

## 7. Model validation

In order to validate the model estimations, the results of kinetic and operation conditions of plant data are compared with the model prediction results. Molar flow rate of components at the output of the process are shown in Table 14. As can be seen, model results have an acceptable agreement with the commercial data. Also, Table 15 presents the plant data and the model predicted temperatures and pressure in the output of each reactor and molecular weight in the output of the process. It can be observed in Tables 14 and 15 that only minor deviations exist between commercial data and calculated results. These minor deviations are due to the two facts. First, the kinetic model used for reaction system of process underestimates the true reaction rate; second, some simplifying assumptions in the mathematical modeling of process are applied.

**Table 12 – Catalyst deactivations model.**

(22)	$r_i = a_i \times r_i^0$	$\left\{ \begin{array}{l} \text{Reaction occurs on acid function} \\ \text{Reaction occurs on metal function} \\ \text{Reaction occurs on acid or metal function} \\ \text{Reaction occurs on acid as well as metal functions} \end{array} \right.$	$a_i = a_A$ $a_i = a_M$ $a_i = \text{mean}(a_A, a_M)$ $a_i = \text{mean}(a_A, a_M)$	
	Reaction occurs on metal function		Reaction occurs on acid function	
(23)	$r_i = a_M \times r_i^0$		(24)	$r_i = a_A \times r_i^0$
(25)	$\frac{da_M}{dC_M} = \alpha_M \times a_M^{n_M}$		(26)	$\frac{da_A}{dC_A} = \alpha_A \times a_A^{n_A}$
(27)	$\left\{ \begin{array}{ll} n_M = 1 & a_M = \exp(-\alpha_M \times C_{C_M}) \\ n_M \neq 1 & a_M = \frac{1}{(1 + (n_M - 1)\alpha_M \times C_{C_M})^{(1/(n_M - 1))}} \end{array} \right.$		(28)	$\left\{ \begin{array}{ll} n_A = 1 & a_A = \exp(-\alpha_A \times C_{C_A}) \\ n_A \neq 1 & a_A = \frac{1}{(1 + (n_A - 1)\alpha_A \times C_{C_A})^{(1/(n_A - 1))}} \end{array} \right.$
(29)	$r_{C_M} = a_{C_M} \times r_{C_M}^0$		(30)	$r_{C_A} = a_{C_A} \times r_{C_A}^0$
(31)	$\frac{da_{C_M}}{dC_{C_M}} = \alpha_{C_M} \times a_{C_M}^{n_{C_M}}$		(32)	$\frac{da_{C_A}}{dC_{C_A}} = \alpha_{C_A} \times a_{C_A}^{n_{C_A}}$
(33)	$\left\{ \begin{array}{ll} n_{C_M} = 1 & a_{C_M} = \exp(-\alpha_{C_M} \times C_{C_M}) \\ n_{C_M} \neq 1 & a_{C_M} = \frac{1}{(1 + (n_{C_M} - 1)\alpha_{C_M} \times C_{C_M})^{(1/(n_{C_M} - 1))}} \end{array} \right.$		(34)	$\left\{ \begin{array}{ll} n_{C_A} = 1 & a_{C_A} = \exp(-\alpha_{C_A} \times C_{C_A}) \\ n_{C_A} \neq 1 & a_{C_A} = \frac{1}{(1 + (n_{C_A} - 1)\alpha_{C_A} \times C_{C_A})^{(1/(n_{C_A} - 1))}} \end{array} \right.$
(35)	$r_{C_M}^0 = \frac{k_{C_M} \times \exp(-E_C/RT)}{P^{n_1} (H_2/H_C)^{n_2}} \times C_{ACP}^{0.5}$		(36)	$r_{C_A}^0 = \frac{k_{C_A} \times \exp(-E_C/RT)}{P^{n_1} (H_2/H_C)^{n_2}} \times C_{ACP}^{0.5}$

## 8. Results and discussion

The process of continuous catalyst regeneration is characterized by high catalyst activity, high quality reformate, and high hydrogen purity. The results of the mathematical modeling for the CCR process are illustrated in the following. The variations of parameters have been investigated in the dimensionless radial and axial coordinates for 3-D plots, also the variations of some parameters have been investigated in 2-D plots.

Results of modeling involve the following main issues in the process:

- Variations of operating conditions.
- Variations of coke concentration and activity of catalyst.
- Variations of molar flow rate of pseudo-components.
- Variations of physical properties.

As can be seen in the results (Tables 14 and 15), satisfactory agreement can be observed between the simulated

**Table 13 – Mass and energy balances and auxiliary relations for CCR process.**

### Mass balance

$$(37) D_{ej} \frac{1}{A_r} \frac{\partial}{\partial r} (A_r \frac{\partial C_j}{\partial r}) - \frac{1}{A_r} \frac{\partial}{\partial r} (A_r u_r C_j) + \rho_b \sum_{i=1}^m a_i \times v_{ij} r_i = \varepsilon \frac{\partial C_j}{\partial t} \quad j = 1, 2, \dots, n \quad i = 1, 2, \dots, m$$

$$(38) \frac{\partial C_j}{\partial r} = -\frac{C_j}{r} - \frac{C_j}{u_r} \frac{\partial u_r}{\partial r} + \frac{\rho_b}{u_r} \sum_{i=1}^m a_i \times v_{ij} r_i \quad j = 1, 2, \dots, n \quad i = 1, 2, \dots, m$$

### Energy balance

$$(39) \frac{1}{A_r} \frac{\partial}{\partial r} (K_{eff} A_r \frac{\partial T}{\partial r}) - \rho_b \left( \sum_{i=1}^m \sum_{j=1}^n (H_j v_{ij}) \times a_i \times r_i \right) - \sum_{j=1}^n N_j \frac{\partial H_j}{\partial r} = \sum_{j=1}^n C_j \frac{\partial U_j}{\partial t} + \varepsilon \sum_{j=1}^n (U_j - H_j) \frac{\partial C_j}{\partial t} \quad j = 1, 2, \dots, n \quad i = 1, 2, \dots, m$$

$$(40) \frac{\partial T}{\partial r} = -\frac{\rho_b}{u_r C_T C_p} \sum_{i=1}^m (\Delta H_i \times a_i \times r_i) \quad i = 1, 2, \dots, m$$

### Velocity distribution

$$(41) \frac{\partial u_r}{\partial r} = -\frac{u_r}{r} - \frac{u_r}{C_T} \times \frac{\partial C_T}{\partial r} + \frac{\rho_b}{C_t} \sum_{j=1}^n \sum_{i=1}^m a_i \times v_{ij} r_i \quad j = 1, 2, \dots, n \quad i = 1, 2, \dots, m$$

### Collector (mass balance)

$$(42) F_{j|z} - F_{j|z+dz} + F_{je} = 0 \quad j = 1, 2, \dots, n$$

$$(43) \frac{\partial F_j}{\partial z} = 2\pi R_i u_{re} C_{je} \quad j = 1, 2, \dots, n$$

### Collector (energy balance)

$$(44) F_T C_p T|_z - F_T C_p T|_{z+dz} + \sum_{j=1}^n F_{je} C_{pe}(T_e - T) = 0$$

$$(45) \frac{\partial T}{\partial z} = -\frac{T}{C_p} \frac{\partial C_p}{\partial z} - \frac{T}{F_T} (2\pi R_i \times u_{re} \times C_{Te}) + \frac{1}{F_T C_p} \times 2\pi R_i \times u_{re} \times C_{Te} \times C_{pe} \times (T_e - T)$$

### Ergun equation (pressure drop)

$$(46) \frac{dp}{dr} = \frac{150\mu}{\phi_s^2 d_p^2} \frac{(1-\varepsilon)^2}{\varepsilon^3} u_r + \frac{1.75\rho}{\phi_s d_p} \frac{(1-\varepsilon)}{\varepsilon^3} u_r^2$$

**Table 14 – Comparison between predicted production rate and plant data.**

Pseudo components	Molecular weight	Input plant (mole fraction)	Output plant (kmol/h)	Output model (kmol/h)	Deviation (kmol/h)
n-P <sub>6</sub> (C <sub>6</sub> H <sub>14</sub> )	86.178	0.0229	71.84	70.98	0.86
n-P <sub>7</sub> (C <sub>7</sub> H <sub>16</sub> )	100.205	0.0292	46.65	46	0.65
n-P <sub>8</sub> (C <sub>8</sub> H <sub>18</sub> )	114.232	0.0239	8.1	7.63	0.47
n-P <sub>9</sub> (C <sub>9</sub> H <sub>20</sub> )	128.259	0.0156	1.15	1.25	-0.1
i-P <sub>6</sub> (C <sub>6</sub> H <sub>14</sub> )	86.178	0.0232	216.06	216.06	0
i-P <sub>7</sub> (C <sub>7</sub> H <sub>16</sub> )	100.25	0.0314	110.18	109.69	0.49
i-P <sub>8</sub> (C <sub>8</sub> H <sub>18</sub> )	114.232	0.0338	22.75	22.67	0.08
i-P <sub>9</sub> (C <sub>9</sub> H <sub>20</sub> )	128.259	0.0244	1.79	1.95	-0.16
ACH <sub>6</sub> (C <sub>6</sub> H <sub>12</sub> )	84.162	0.0077	0.51	0.92	-0.41
ACH <sub>7</sub> (C <sub>7</sub> H <sub>14</sub> )	98.189	0.0084	0.92	1.43	-0.51
ACH <sub>8</sub> (C <sub>8</sub> H <sub>16</sub> )	112.216	0.0115	2.33	2.34	-0.01
ACH <sub>9</sub> (C <sub>9</sub> H <sub>18</sub> )	126.243	0.0018	0.04	0.05	-0.01
ACP <sub>5</sub> (C <sub>5</sub> H <sub>10</sub> )	70.135	0.0001	2.14	2.11	0.03
ACP <sub>6</sub> (C <sub>6</sub> H <sub>12</sub> )	84.162	0.003	26	26.02	-0.02
ACP <sub>7</sub> (C <sub>7</sub> H <sub>14</sub> )	98.189	0.0065	2.33	3.12	-0.79
ACP <sub>8</sub> (C <sub>8</sub> H <sub>16</sub> )	112.216	0.0084	0.6	0.6	0
ACP <sub>9</sub> (C <sub>9</sub> H <sub>18</sub> )	126.243	0.0012	0.01	0.02	-0.01
A <sub>6</sub> (C <sub>6</sub> H <sub>6</sub> )	78.114	0.0086	205.84	206.39	-0.55
A <sub>7</sub> (C <sub>7</sub> H <sub>8</sub> )	92.141	0.0109	453.93	454.33	-0.4
A <sub>8</sub> (C <sub>8</sub> H <sub>10</sub> )	106.168	0.0021	163.02	163.47	-0.45
A <sub>9</sub> (C <sub>9</sub> H <sub>12</sub> )	120.195	0.0026	323.66	324.46	-0.8
A <sub>8</sub> (C <sub>8</sub> H <sub>10</sub> )	106.168	0.0015	113.62	113.4	0.22
A <sub>8</sub> (C <sub>8</sub> H <sub>10</sub> )	106.168	0.0016	120.84	121.55	-0.71
A <sub>8</sub> (C <sub>8</sub> H <sub>10</sub> )	106.168	0.0036	276.56	276.8	-0.24
H <sub>2</sub>	2.016	0.6226	10071.31	10090.82	-19.51
P <sub>1</sub> (CH <sub>4</sub> )	16.043	0.0211	398.53	396.64	1.89
P <sub>2</sub> (C <sub>2</sub> H <sub>6</sub> )	30.07	0.0231	399.16	397.72	1.44
P <sub>3</sub> (C <sub>3</sub> H <sub>8</sub> )	44.097	0.0202	352.36	351.69	0.67
P <sub>4</sub> (C <sub>4</sub> H <sub>10</sub> )	58.124	0.0106	189.21	189.93	-0.72
P <sub>5</sub> (C <sub>5</sub> H <sub>12</sub> )	72.151	0.0035	71.06	71.69	-0.63
i-P <sub>4</sub>	58.124	0.0073	140.75	139.38	1.37
i-P <sub>5</sub>	72.151	0.0076	149.21	149.49	-0.28

results and commercial values. Thus, the proposed model predicts the reactor and catalyst performance and quality of reformate very well. Some variables such as feedstock properties, temperature and pressure of reaction, space velocity, and hydrogen over hydrocarbon molar ratio, affect the enhancement of main products yield and reactor performance (Pisayorius, 1985). Since the operating conditions (pressure and temperature) of process side play a significant role in the performance of the catalyst as well as the yield and quality of reformate, these variables have been investigated firstly.

### 8.1. Investigation of operating conditions during the process

In this section, variation of operating conditions (pressure and temperature) in CCR process is investigated. One of the advantages of the CCR process is the negligible pressure drop in the reactors, which allows the use of smaller catalyst particles with higher efficiency. As shown in Fig. 6a, the variations of pressure inside the reactors are slight, and sudden drops are

observed during the passage of a stream through one reactor to another due to piping and instruments such as a furnace.

In order to consider the variation of temperature in catalytic naphtha reforming, the temperature profile of the plant is depicted in Fig. 6b. In this 3-D plot, temperature vs. dimensionless radial and axial coordinates of reactor is illustrated. Since the major reforming reactions are highly endothermic, temperature decreases by proceeding of the reactions, and then production rate of reactions decrease. Consequently, to maintain the reaction temperature at suitable level, commercial catalytic reformers are designed with multiple reactors and intermediate furnaces. In the first reactor, naphthenes concentration are high and dominant reaction in this reactor (dehydrogenation) is very fast and endothermic, thus, it causes a very sharp temperature drop in the radial direction in the first reactor, which is demonstrated in Fig. 6b. Due to the remarkable decrease in the temperature of first reactor, the outlet stream of the first reactor is preheated via a furnace to the same entrance temperature of the first reactor and then is sent to the second reactor. In the second

**Table 15 – Comparison between predicted temperature, pressure and molecular weight with plant data.**

Reactor number	Outlet temperature		Outlet pressure		Outlet molecular weight	
	Plant	Model	Plant	Model	Plant	Model
1	707	710.7	581	585.1	–	–
2	725	726.4	535	540.3	–	–
3	743	743.2	490	495.7	–	–
4	761	758.9	446	451.4	21.9	21.87

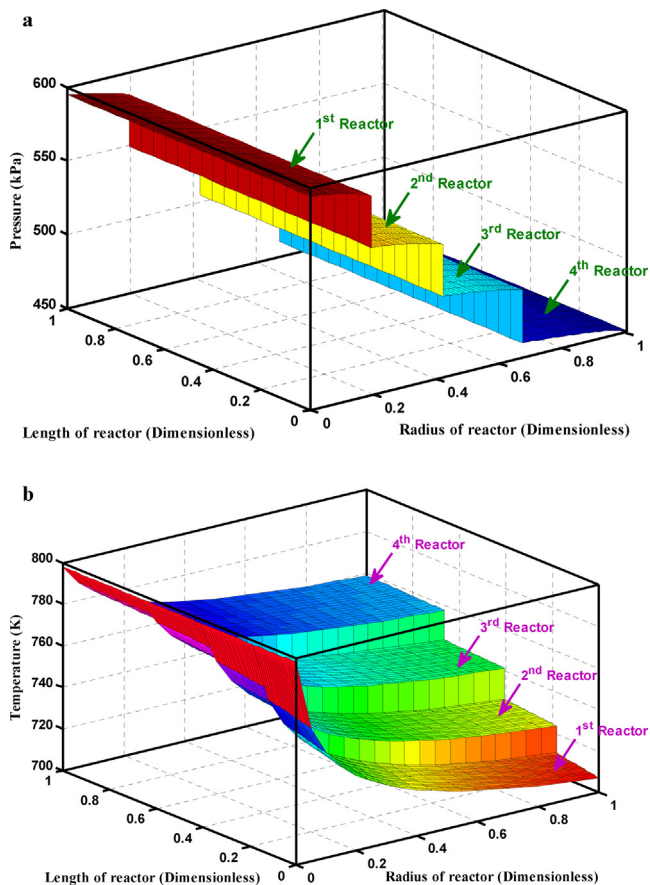


**Fig. 6 – Changes of (a) temperature and (b) pressure during the process.**

reactor, remaining naphthenes take part in the dehydrogenation reaction. But, due to the decrease in the amount of naphthenes in this reactor, the lower dehydrogenation reaction occurs, thus temperature drop decreases. In order to compensate temperature reduction, the effluent stream of the second reactor is preheated again and then is sent to the third reactor. Reduction in the temperature drop also can be observed in the third reactor. In this reactor, dehydrocyclization of paraffins (endothermic reaction) decreases the temperature, but hydrocracking of naphthenes and paraffins (exothermic reactions) increase temperature. Thus moderate temperature drop is achieved in the third reactor. The lowest temperature reduction is observed in the last reactor. In this reactor dehydrocyclization of paraffins to naphthenes and dehydrogenation of naphthenes to aromatics which are endothermic reactions, cause temperature drop, while exothermic reactions in this reactor (hydrodealkylation and hydrocracking reactions) have more effect than the previous reactors. Consequently, the average temperature in the last reactor is higher than the first ones. As can be seen in Fig. 6b, temperature increases very slightly in the axial direction (length) of the reactors. These increases are due to deactivation of catalyst in this direction, and consequently, reactions rate decrease and temperature increases.

## 8.2. Catalyst investigation

In the CCR operation, the amount of deposited coke on the catalyst must be kept at a low level to maintain reasonable activity, proper regenerator performance and high-purity products. As previously mentioned, the catalyst affects the

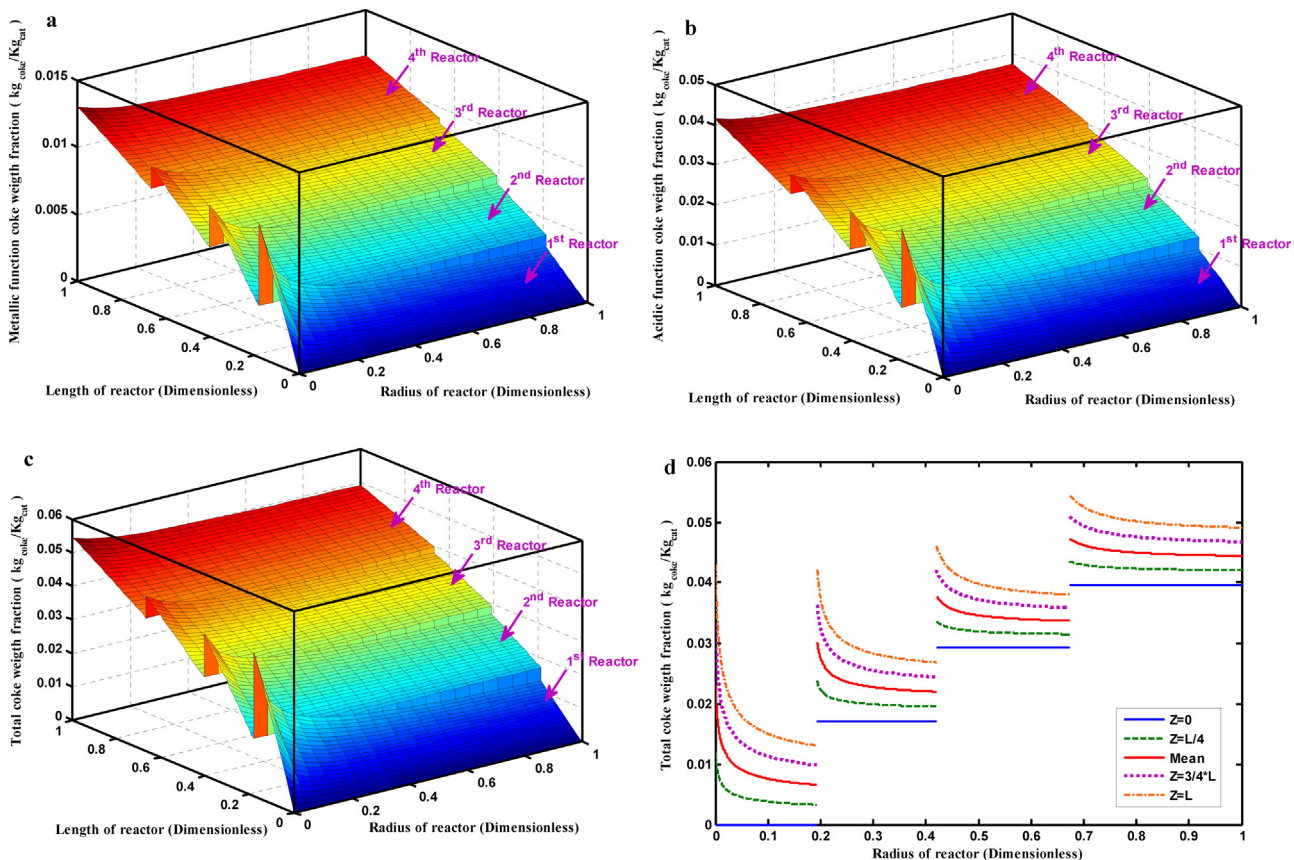
reaction rates through its two different functions: metallic and acidic (Carter et al., 1982), which coke can be formed on the both of them. This coke causes a decrease in the activity of the catalyst.

Fig. 7 depicts coke weight fraction distribution in the metallic and acidic functions and total amount (sum of both) in the axial and radial directions for the CCR process. Coke distribution is plotted as a function of dimensionless radial and axial coordinates. Fig. 7a illustrates coke weight fraction distribution in the metallic function along the four reactors in this process. As can be seen, the variations in the coke content are in the radial and axial directions in all of the reactors. In the radial direction the largest coke content occurs at the entrance of each reaction side ( $R = R_{\text{input}}$ ), because high temperature, relatively high alkylcyclopentane concentration and the low ratio of  $H_2/HC$  exist in the entrance of reaction side. In addition, due to reduction of temperature and alkylcyclopentane concentration as well as increase of  $H_2/HC$  ratio, and according to the coke formation rate (Eq. (17)), coke formation decreases in this direction. In the axial direction of reactors, catalyst moves downward in the reaction side with gravity and due to the occurrence of reactions in each site, coke deposits on the catalyst surface and deactivation of catalyst take place. After passing from this site and transferring to the next site, the new coke is deposited to the catalyst. Consequently, this trend continues to bottom of reactor. The same trend is observed for coke weight fraction distribution in the acidic function in Fig. 7b. Total coke content in the process is equal the sum of coke content in the metallic and acidic functions, as shown in Fig. 7c. In addition, total coke content vs. radius of reactors in various lengths of each reactor is depicted in a two-dimensional plot in Fig. 7d. According to the commercial data, coke weight fraction in the output of fourth reactor is .05. As can be seen in Fig. 7c and d, acceptable agreement can be observed between simulated and commercial values.

The catalyst activity in the CCR process is illustrated in Fig. 8. The variations of catalyst activity are inversely related to the coke weight fraction distribution in the process. Thus, by enhancement of coke deposition, catalyst activity decreases. In order to investigate the catalyst activity, metallic and acidic functions activities are plotted as a function of dimensionless radius in the various lengths of the reactors in Fig. 8a and b, respectively. As previously discussed, in the radial direction of reactors, reduction of coke deposition can be seen, also in the axial direction, coke formation increases. Consequently, according to the inverse relation of coke formation and catalyst activity, enhancement of catalyst activity in the radial direction and reduction in the axial direction can be observed.

## 8.3. Effects and changes of $H_2/HC$ molar ratio

Hydrogen over hydrocarbon molar ratio is one of the key parameters in the naphtha reforming process. As previously mentioned, coke deposition on the catalyst surface has a major role in the catalyst deactivation. A proper  $H_2/HC$  molar ratio enhances the catalyst life time and keeps the catalyst safe from the coke formation and deactivation; so it has effect on the appropriate production of hydrogen and aromatics. In Fig. 9, the 3-D plot of  $H_2/HC$  molar ratio vs. the radial and axial coordinates of reactor is illustrated. As can be seen, the  $H_2/HC$  molar ratio increases continuously in the radial direction, and ascending trend is observed for the  $H_2/HC$  molar ratio in the process due to continuous production of hydrogen.



**Fig. 7 – Coke concentration distribution in (a) metallic function, (b) acidic function and (c) total coke. (d) comparison coke content in various length of reactors.**

#### 8.4. Pseudo-components

As previously discussed, the proposed kinetic model is based on 32 pseudo-components, and naphtha feed has been characterized by naphthenes (alkyl-cyclohexenes: ACH, alkyl-cyclopentanes: ACP), paraffins (normal paraffins: NP, iso paraffins: IP), and aromatics (A) lumps. One of the main aims in the naphtha reforming process is the production of aromatic components such as benzene, toluene and xylene (BTX), by consuming paraffins and naphthenes. In this section, the variations of molar flow rate of pseudo-components have been investigated along the dimensionless radial and axial coordinates. In this coordinates, in the radial direction, for any radius, mean variations of molar flow rate in the axis is considered. Also, the variations of molar flow rate of pseudo-components along the length of collector (annulus) are illustrated by solid lines.

Naphthene has a main role in the reforming process because high octane number of reformate can be obtained by transformation of naphthenes to aromatics. In this study, naphthene has been considered in two categories, including alkyl-cyclohexane (ACH) and alkyl-cyclopentane (ACP). The variations of alkyl-cyclohexane during the process are depicted in Fig. 10a. Molar flow rate of ACH in the radial direction decreases, because it takes part in the dehydrogenation and hydrocracking reactions. In the second reactor, reduction of ACH is lower than the first one, because the occurrence of isomerization reactions (moderately fast reactions), that produce ACH, in this reactor is more than the first one. In addition, in the last two reactors, dehydrocyclization reactions produce more ACH than the first two ones, thus, consumption rate of ACH is lower in these reactors. The variations of ACP in

the process depend on the isomerization, hydrocracking and dehydrocyclization reactions. As shown in Fig. 10b, in the radial direction the amount of ACP decreases as a result of isomerization and hydrocracking reactions, but in the last two reactors, due to the production of ACP in the dehydrocyclization reaction, consumption rate decreases. Variations of molar flow rate of naphthenes (ACH and ACP) along the length of annulus are shown by solid lines in Fig. 10a and b. Unreacted naphthenes accumulate along the length of annulus, and then at the bottom of reactor are sent to the next reactor to take part in the new reactions, thus, molar flow rate decreases during the process.

Paraffins have a similar behavior to the naphthenes in the reforming process. Paraffins, as one of the main reactants in the naphtha reforming process, lead to higher aromatics production rate. The variations of n-paraffins and iso-paraffins in the process are shown in Fig. 11. As can be seen in Fig. 11a, molar flow rate of n-paraffins, due to being of the dehydrocyclization, hydrocracking and isomerization reactions decrease along the radius of reactors (dotted curve). As shown in Fig. 11b, iso-paraffins have a similar trend to n-paraffins, but consumption of NPs due to isomerization reactions are more than the IPs. The variations of paraffins (normal and iso) along the length of annulus have a similar pattern to the naphthenes variations in the CCR process that are illustrated in Fig. 11a and b by solid lines.

In the naphtha reforming process, aromatics are the main products. The considered aromatics in the proposed kinetic model are: benzene, toluene, xylene (BTX), ethylbenzene and heavy aromatics ( $A_9^+$ ). One of the main byproduct in this process is hydrogen. In the following, the variations of these pseudo-components are investigated. Aromatics with eight

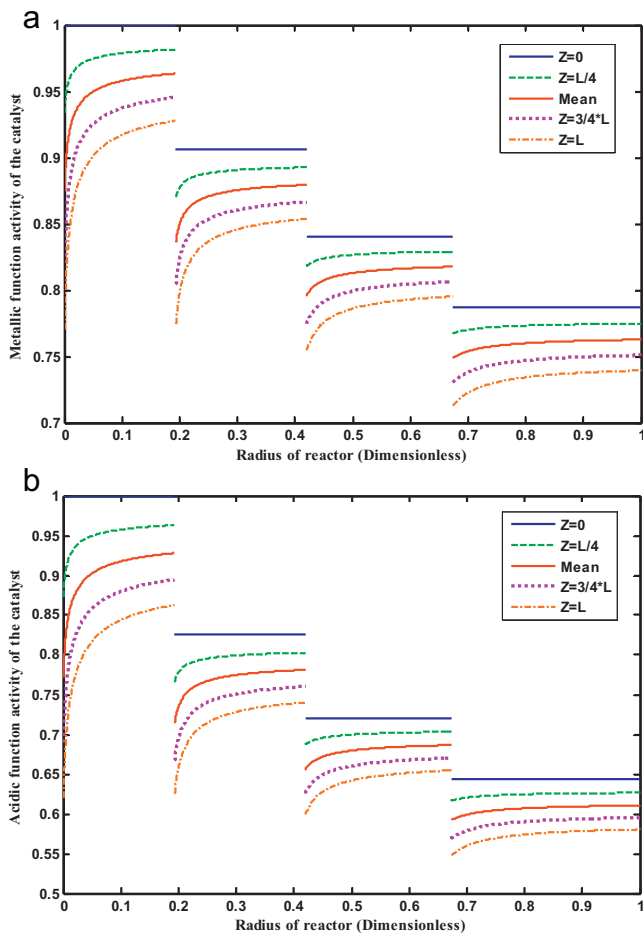


**Fig. 8 – Catalyst activity in (a) metallic function and (b) acidic function.**

carbon atoms such as ethylbenzene, and ortho-, meta-, and para-xylene are depicted in Fig. 12a, and aromatics with six and seven carbon atoms, also heavy aromatics ( $A_9^+$ ) are shown in Fig. 12b. Aromatics molar flow rate except heavy aromatics ( $A_9^+$ ), during the process have a similar pattern. As can be seen in Fig. 12a and b, aromatics are produced along the radius of reactor, but production rate in the first two reactors is more than the last two reactors, because dehydrogenation as a fast reaction occurs mostly in the first two reactors that produces aromatic components. Also, heavy aromatics ( $A_9^+$ ) have similar conditions, but in the last reactor due to consumption of heavy aromatics in the slow reactions (hydrodealkylation

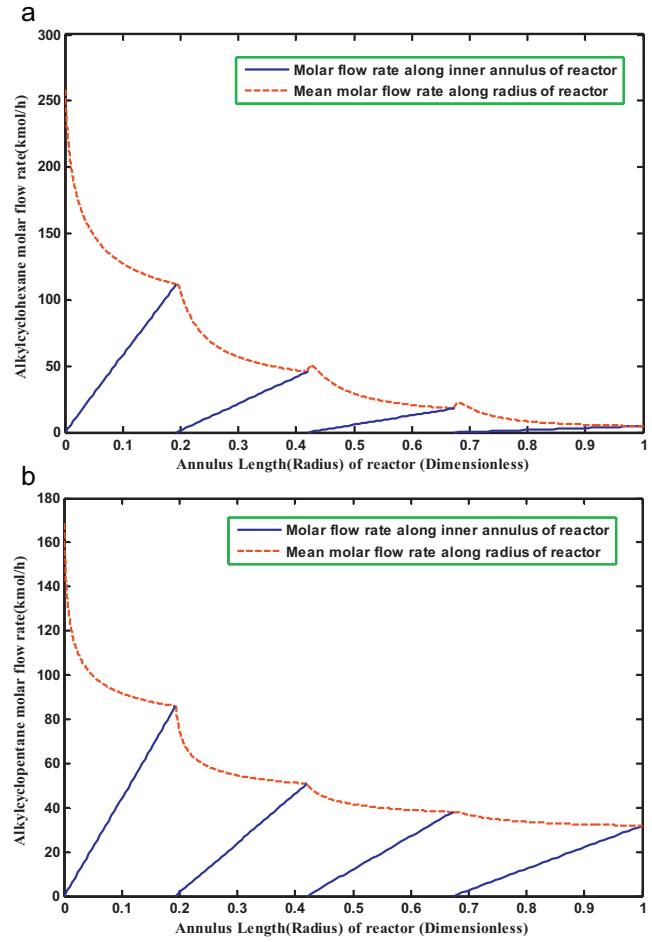


**Fig. 10 – Variations of molar flow rate of (a) alkyl-cyclohexane and (b) alkyl-cyclopentane in the process.**

reactions, such as  $r_{1691-1}$  and  $r_{169-2}$ ), molar flow rate decreases. Aromatics molar flow rate along the length of collector is shown by solid lines in Fig. 12a and b. Produced aromatics in the reactor collect in the annulus, and then, are sent to the next reactor. In the next reactor, aromatics production continues. Thus, as shown in Fig. 12a and b by solid lines, molar flow rate of aromatics increases during the process.

Hydrogen, as a main byproduct in the reforming process, has a dual role in the naphtha reforming as a product and reactant. It acts as a product in the dehydrogenation and dehydrocyclization reactions and as a reactant in the hydrodealkylation and hydrocracking reactions. But total hydrogen during the process increases because its production rate is more than the consumption rate. As shown in Fig. 13, hydrogen molar flow rate increases during the process but production rate decreases, because, as previously discussed, hydrodealkylation and hydrocracking reactions, as slow reactions, take place in the last two reactors. Other products in the naphtha reforming process are light ends that have a main role in the refineries. Light ends are produced in the hydrocracking reactions that occur in all reactors. But, owing to these reactions take place mostly in the last two reactors, production rate of light ends increases in these reactors, as shown in Fig. 14.

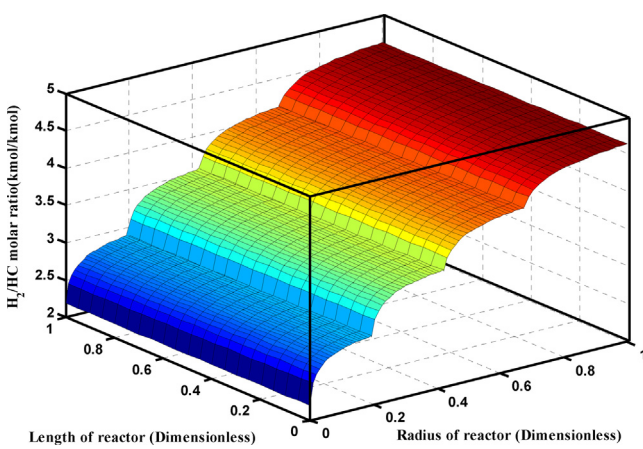


**Fig. 9 – The H<sub>2</sub>/HC molar ratio in the CCR process.**

### 8.5. Physical properties

In this study, physical properties such as heat capacity, viscosity and molecular weight are considered as variable

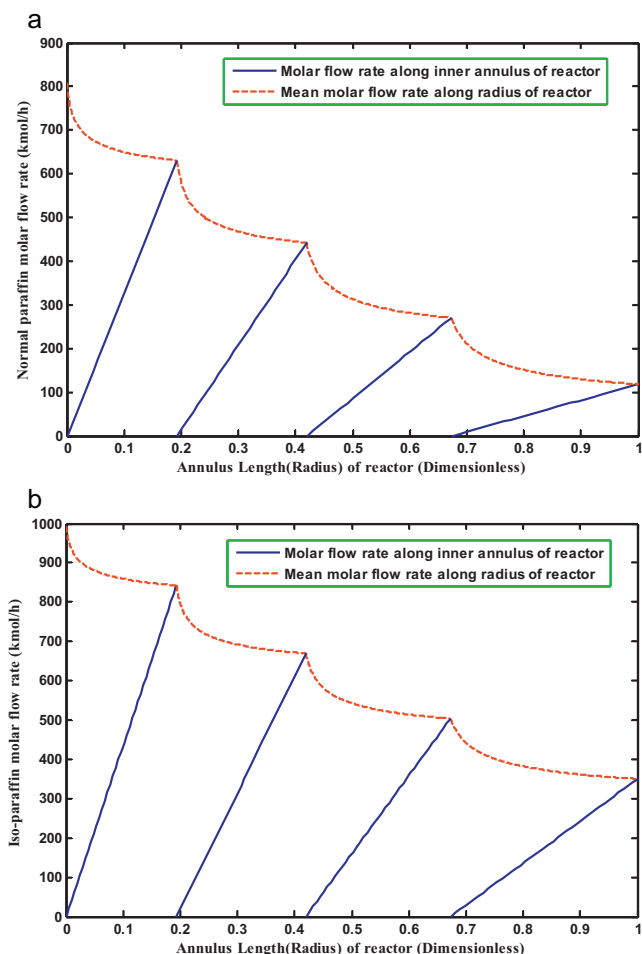


**Fig. 11 – Variations of molar flow rate of (a) normal-paraffin and (b) iso-paraffin in the process.**

parameters. In this section, variations of these physical properties are illustrated in radial coordinates. Heat capacity variations, is depicted in Fig. 15a. As previously mentioned, the major reforming reactions are highly endothermic, thus, temperature decreases in radial direction and due to direct relationship between heat capacity and temperature, heat capacity decreases in the reactors. As can be seen in Fig. 15a, at the entrance of reactors heat capacity is high due to high temperature, but endothermic reactions in the reactors cause temperature drop. Consequently, reduction of heat capacity can be observed in each reactor. The outlet stream of reactors is preheated via a furnace that causes sudden jumps in the heat capacity plot. During the process, increase of temperature has a positive effect on the heat capacity, but due to production of hydrogen, which has a very low heat capacity in comparison of other components, downward trend occurs.

In the viscosity behavior, dominant agent is temperature of components. Thus, during the process, the trend of viscosity obeys temperature conditions. As shown in Fig. 15b, viscosity decreases along the radius of reactors due to temperature reduction, and an ascendant trend can be observed during the process, because the outlet stream of reactors is heated by the furnace. One of the other significant physical properties in the naphtha reforming process is molecular weight, which is affected by proceeding of the reactions. In Fig. 15c, molecular weight is depicted vs. radius of reactors. Molecular weight decreases in the radial direction due to proceeding of reactions and produce light products such as hydrogen and light ends.

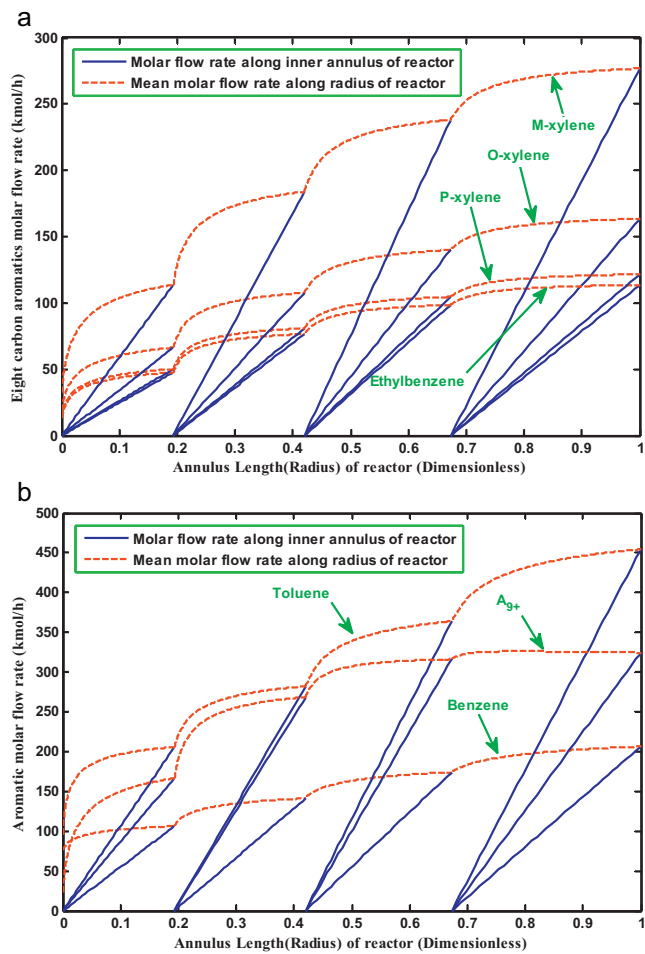


**Fig. 12 – Molar flow rate of (a) aromatics with eight carbon atoms and (b) Toluene, Benzene and heavy aromatics with  $A_{9+}$ .**

#### 8.6. Superficial velocity

The superficial gas velocity is one of the key parameters in design and operation of various moving bed reactors, from an engineering viewpoint. As the gas volumetric flow rate is divided by the cross-sectional area, it is defined according to Eq. (47):

$$U_r = \frac{Rm \cdot T}{PMA} \quad (47)$$

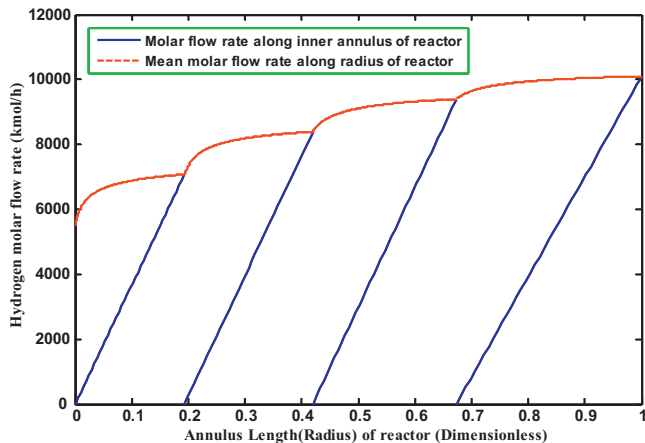


**Fig. 13 – Molar flow rate of hydrogen in the CCR process.**

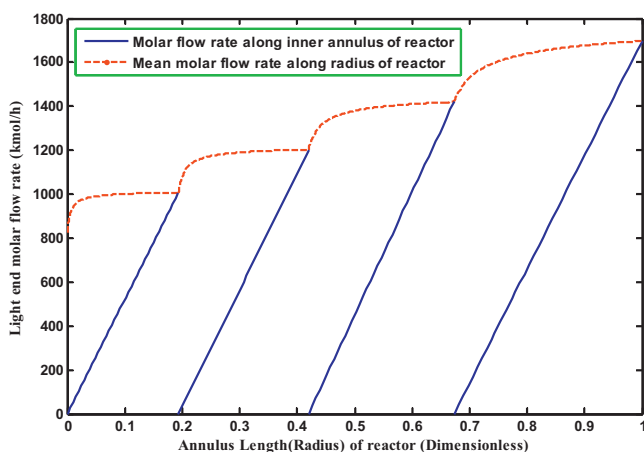


Fig. 14 – Molar flow rate of light end.

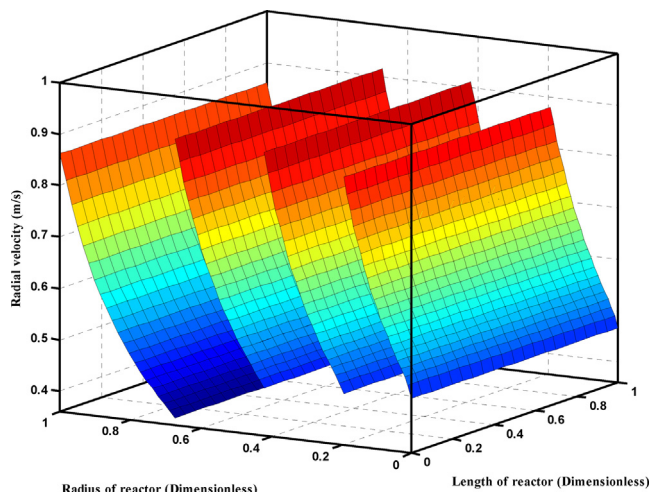


Fig. 16 – Superficial velocity in the reforming process.

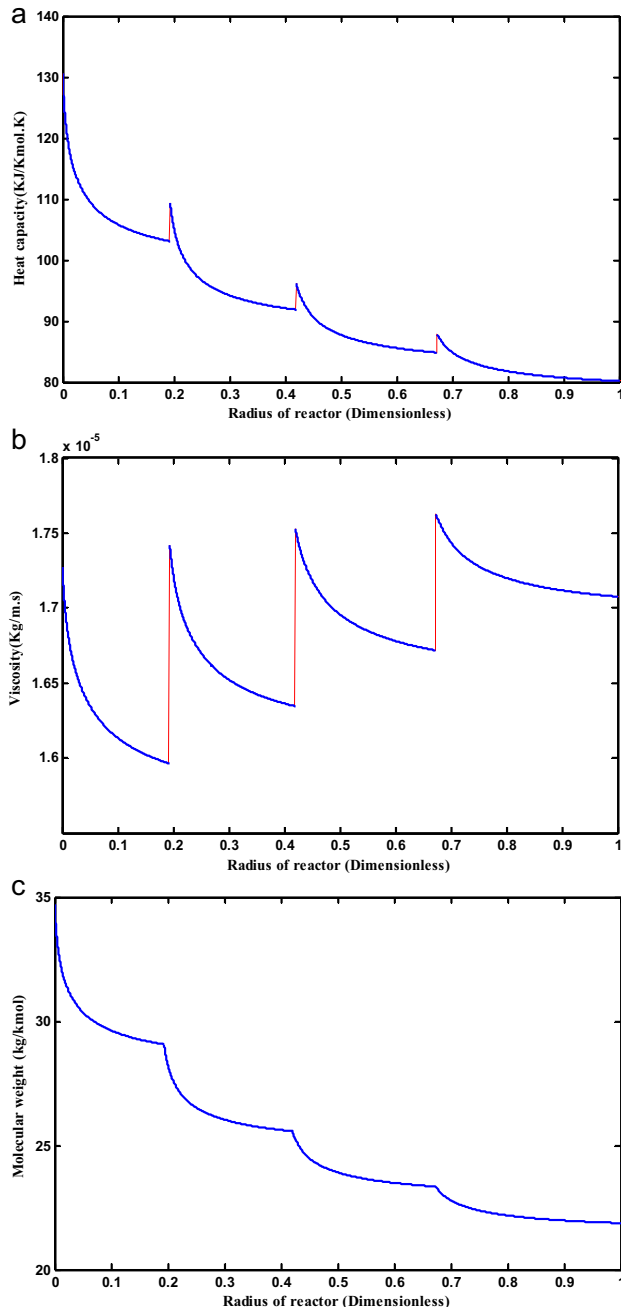


Fig. 15 – Physical properties in the process (a) heat capacity (b) viscosity (c) molecular weight.

Superficial velocity can be varied with the changes of temperature (T), pressure (P), molecular weight (M) or cross section area (A) at various radial positions. But superficial gas velocity almost is unchanged at various axial locations because in the axial direction the temperature and pressure gradient are very small, cross section area is constant, and molecular weight is almost unchanged in this direction. Consequently, superficial velocity along the various lengths of reaction side in each radius is nearly constant. As shown in 3-D plot in Fig. 16, in the radial direction, superficial velocity increases, because in this direction pressure, temperature, molecular weight and cross section area decrease. Although diminution in temperature causes reduction of superficial velocity, but the effect of decrease in molecular weight, cross section area and pressure are more. Consequently, according to Eq. 47, superficial velocity increases in the radial direction. Auxiliary correlations of velocity distribution are presented in Appendix D.

## 9. Conclusions

Catalytic reforming is one of the key processes in the refinery to produce high-octane gasoline, aromatics and hydrogen as a clean fuel. In this study, mathematical modeling of continuous catalytic regeneration in the naphtha reforming unit has been developed. This model includes a new kinetic model for the catalytic naphtha reforming with 32 pseudo components and 84 reactions. In addition, a new model for the catalyst deactivation rate, by considering cross flow pattern in the reactors, is presented. Some variables such as reaction temperature and pressure, superficial velocity, and hydrogen to hydrocarbon molar ratio (Antos and Aitani, 1995) have effect on the performance of the catalytic naphtha reforming process. In this work, variations of these parameters along the radial and axial directions of reactors, also the variations of proposed pseudo components in the reforming process have been investigated. Acceptable agreement has been obtained between commercial values and simulated results of the molar flow rate of pseudo components, coke content of catalysts, operating conditions and physical properties which indicate the acceptable prediction ability of the proposed kinetic model.

## Appendix A. Catalyst deactivation model

Reaction rate of pseudo-components based on activity of catalyst and reaction rate on the fresh catalyst can be obtained by:

$$r_i = a_i \times r_i^0 \quad (A1)$$

Then, by considering catalyst function for each reaction,

$$\begin{cases} \text{Reaction occurs on acidic function} & a_i = a_A \\ \text{Reaction occurs on metallic function} & a_i = a_M \\ \text{Reaction occurs on acidic or metallic function} & a_i = \text{mean}(a_A, a_M) \\ \text{Reaction occurs on acidic as well as metallic functions} & a_i = \text{mean}(a_A, a_M) \end{cases}$$

Thus, the rate of reaction that is catalyzed by metallic function could be written as:

$$r_i = a_M \times r_i^0 \quad (A2)$$

Also, metallic function activity ( $a_M$ ) is a function of deposited coke weight fraction on the metallic function of catalyst, which could be calculated by:

$$-\frac{da_M}{dC_{CM}} = \alpha_M \times a_M^{n_M} \quad (A3)$$

where  $\alpha_M$  is a constant and  $n_M$  is a power number of metallic function activity.  $\alpha_M$  and  $n_M$  must be determined via minimization of difference between plant data and modeling output. Then With integration of recent equation, we have:

$$\begin{cases} \text{If } n_M = 1 \quad a_M = \exp(-\alpha_M \times C_{CM}) \\ \text{If } n_M \neq 1 \quad a_M = \frac{1}{(1 + (n_M - 1)\alpha_M \times C_{CM})^{(1/(n_M - 1))}} \end{cases} \quad (A4)$$

In the above equation  $C_{CM}$  is coke weight fraction on the metallic function that the following coke balance on the metallic function along the Z direction is applied for its calculation:

$$F_{CM}|_z - F_{CM}|_{z+dz} + r_{CM} \times (\rho_B \times 2 \times \pi \times r \times \Delta r \times dz) = 0 \quad (A5)$$

By considering the Taylor's extension, the above equation becomes:

$$\frac{\partial F_{CM}}{\partial z} = r_{CM} \times (\rho_B \times 2 \times \pi \times r \times \Delta r) \quad (A6)$$

where  $F_{CM}$  and  $r_{CM}$ , are mass flow rate of coke and rate of coke formation on the metallic function of catalyst. In addition,  $F_{CM}$  can be defined as:

$$F_{CM} = C_{CM} \times \dot{m}_{Cat.} \quad (A7)$$

Also, mass flow rate of catalyst is defined by:

$$\dot{m}_{Cat.} = \rho_b \times 2 \times \pi \times r \times \Delta r \times u_z \quad (A8)$$

By substituting the above equation in Eq. (A7):

$$F_{CM} = C_{CM} \times (\rho_b \times 2 \times \pi \times r \times \Delta r \times u_z) \quad (A9)$$

Then, Eq. (A9) is replaced in Eq. (A6):

$$u_z \frac{\partial C_{CM}}{\partial z} = r_{CM} \quad (A10)$$

By rearranging above equation, we have:

$$\frac{\partial C_{CM}}{\partial z} = \frac{r_{CM}}{u_z} \quad (A11)$$

Thus, the coke weight fraction on the metallic function ( $C_{CM}$ ), depends on the rate of coke formation on the metallic function of spent catalyst ( $r_{CM}$ ) and catalyst velocity ( $u_z$ ). Therefore to solve Eq. (A11), the rate of coke formation must be calculated:

$$r_{CM} = a_{CM} \times r_{CM}^0 \quad (A12)$$

$r_{CM}^0$  is rate of coke formation on the metallic function of fresh catalyst, which is defined by:

$$r_{CM}^0 = \frac{k_{CM} \times \exp(-E_c/RT)}{P^{n_1} (H_2/HC)^{n_2}} \times C_{ACP}^{0.5} \quad (A13)$$

In addition,  $a_{CM}$  could be calculated by:

$$-\frac{da_{CM}}{dC_{CM}} = \alpha_{CM} \times a_{CM}^{n_{CM}} \quad (A14)$$

$n_{CM}$  and  $\alpha_{CM}$  similar to unknown constants of Eq. (A3), must be determined via minimization of difference between plant data and modeling output. With integration from Eq. (A14), we have:

$$\begin{cases} \text{If } n_{CM} = 1 \quad a_{CM} = \exp(-\alpha_{CM} \times C_{CM}) \\ \text{If } n_{CM} \neq 1 \quad a_{CM} = \frac{1}{(1 + (n_{CM} - 1)\alpha_{CM} \times C_{CM})^{(1/(n_{CM} - 1))}} \end{cases} \quad (A15)$$

To calculate the rate of coke formation on the metallic function Eqs. (A15) and (A13) must be replaced in Eq. (A12), then by substituting coke formation rate in Eq. (A11), coke weight fraction on the metallic function ( $C_{CM}$ ) could be calculated. With same procedure, the rate of reactions that are catalyzed by acidic site could be achieved, the results shown in Table 12. In addition, required constants to calculate catalyst deactivation rate and activity are presented in Table A.1.

## Appendix B. Developing of governing equations

### B.1. Mass balance

To develop the mathematical model the derivation of governing equations (mass and energy balances) have been discussed here. The mass balance for a control volume with length of  $dz$  and cross section area of  $A$  is:

$$\text{Input} - \text{Output} + \text{Consumption} = \text{Accumulation} \quad (B1)$$

**Table A.1 – Require constants to calculate catalyst deactivation rate.**

Parameter	Value	Dimension
$n_M$	1	–
$\alpha_M$	26	$\frac{\text{kg}_{\text{cat}}}{\text{kg}_{\text{coke}}}$
$n_{C_M}$	1	–
$\alpha_{C_M}$	12.34	$\frac{\text{kg}_{\text{cat}}}{\text{kg}_{\text{coke}}}$
$n_A$	1	–
$\alpha_A$	14.5	$\frac{\text{kg}_{\text{cat}}}{\text{kg}_{\text{coke}}}$
$n_{C_A}$	1	–
$\alpha_{C_A}$	10.18	$\frac{\text{kg}_{\text{cat}}}{\text{kg}_{\text{coke}}}$
$k_{C_M}$	0.384	$\frac{\text{kg}_{\text{coke}} \times (\text{kPa})^{n_1} \text{m}^{1.5}}{\text{kg}_{\text{cat}} (\text{kmol})^{0.5}}$
$k_{C_A}$	1.386	$\frac{\text{kg}_{\text{coke}} \times (\text{kPa})^{n_1} \text{m}^{1.5}}{\text{kg}_{\text{cat}} (\text{kmol})^{0.5}}$
$E_c$	4055	$\frac{\text{J}}{\text{mol}}$
$n_1$	0.94	–
$n_2$	1.33	–

$$(N_j \times A_r)|_r - (N_j \times A_r)|_{r+dr} + \rho_b \sum_{i=1}^m a_i \times v_{ij} r_i \times A_r \times dr = \frac{\partial n_j}{\partial t} \quad j = 1, 2, \dots, n \quad i = 1, 2, \dots, m \quad (B2)$$

where  $n_j$  is mole of component  $j$  in control volume and  $N_j$  is molar flux of component  $j$ , by writing the Taylor's extension of second term in left hand of mass balance equation, is obtained:

$$-\frac{\partial(N_j \times A_r)}{\partial r} \cdot dr + \rho_b \sum_{i=1}^m a_i \times v_{ij} r_i \times A_r \times dr = \frac{\partial n_j}{\partial t} \quad (B3)$$

Then, by dividing the above equation over the volume of the differential element:

$$-\frac{1}{A_r} \frac{\partial(N_j \times A_r)}{\partial r} + \rho_b \sum_{i=1}^m a_i \times v_{ij} r_i = \frac{1}{A_r \times dr} \frac{\partial n_j}{\partial t} \quad (B4)$$

To simplify the above equation, by considering concentration of component  $j$  in control volume:

$$C_j = \frac{n_j}{(A_r \times dr \times \varepsilon)} \quad (B5)$$

Or

$$n_j = C_j \times (A_r \times dr \times \varepsilon) \quad (B6)$$

Cross section area is obtained as follows:

$$A_r = 2\pi r \times dz \quad (B7)$$

By applying the above equations one can obtain:

$$-\frac{1}{A_r} \frac{\partial(N_j \times A_r)}{\partial r} + \rho_b \sum_{i=1}^m a_i \times v_{ij} r_i = \varepsilon \frac{\partial C_j}{\partial t} \quad (B8)$$

The molar flux comprises two terms, ones due to the bulk motion and the other one for diffusion of component  $j$  as follows:

$$N_j = -D_{ej} \frac{\partial C_j}{\partial r} + C_j u_r \quad (B9)$$

or

$$N_j A_r = -A_r D_{ej} \frac{\partial C_j}{\partial r} + A_r C_j u_r \quad (B10)$$

By substituting the above equation in Eq. (B8), we have:

$$D_{ej} \frac{1}{A_r} \frac{\partial}{\partial r} (A_r \frac{\partial C_j}{\partial r}) - \frac{1}{A_r} \frac{\partial}{\partial r} (A_r u_r C_j) + \rho_b \sum_{i=1}^m a_i \times v_{ij} r_i = \varepsilon \frac{\partial C_j}{\partial t} \quad j = 1, 2, \dots, n \quad i = 1, 2, \dots, m \quad (B11)$$

The CCR process is steady state, and diffusion in comparison to bulk motion is negligible, thus:

$$-\frac{1}{A_r} \frac{\partial}{\partial r} (A_r u_r C_j) + \rho_b \sum_{i=1}^m a_i \times v_{ij} r_i = 0 \quad j = 1, 2, \dots, n \quad i = 1, 2, \dots, m \quad (B12)$$

To simplify this equation, the following relation is used:

$$\begin{aligned} -\frac{1}{A_r} \frac{\partial}{\partial r} (A_r u_r C_j) &= -\frac{u_r C_j}{A_r} \frac{\partial A_r}{\partial r} - u_r \frac{\partial C_j}{\partial r} - C_j \frac{\partial u_r}{\partial r} \\ &= -\frac{u_r C_j}{r} - u_r \frac{\partial C_j}{\partial r} - C_j \frac{\partial u_r}{\partial r} \end{aligned} \quad (B13)$$

By substituting recent equation in Eq. (B12):

$$-\frac{u_r C_j}{r} - u_r \frac{\partial C_j}{\partial r} - C_j \frac{\partial u_r}{\partial r} + \rho_b \sum_{i=1}^m a_i \times v_{ij} r_i = 0 \quad j = 1, 2, \dots, n \quad i = 1, 2, \dots, m \quad (B14)$$

Consequently, final equation of mass balance in the CCR process obtains:

$$\frac{\partial C_j}{\partial r} = -\frac{C_j}{r} - \frac{C_j}{u_r} \frac{\partial u_r}{\partial r} + \frac{\rho_b}{u_r} \sum_{i=1}^m a_i \times v_{ij} r_i \quad j = 1, 2, \dots, n \quad i = 1, 2, \dots, m \quad (B15)$$

## B.2. Energy balance

Energy balance in the CCR process is obtained by applying the first law of thermodynamic:

$$\begin{aligned}
 \left( \begin{array}{c} \text{Rate of} \\ \text{accumulation} \\ \text{of energy} \\ \text{within the} \\ \text{system} \end{array} \right) &= \left( \begin{array}{c} \text{Rate of} \\ \text{energy added} \\ \text{to the system} \\ \text{by conduction} \\ \text{heat transfer} \end{array} \right) + \left( \begin{array}{c} \text{Rate of} \\ \text{energy leaving} \\ \text{the system} \\ \text{by conduction} \\ \text{heat transfer} \end{array} \right) \\
 &+ \left( \begin{array}{c} \text{Rate of} \\ \text{work done} \\ \text{by the} \\ \text{system on the} \\ \text{surroundings} \end{array} \right) + \left( \begin{array}{c} \text{Rate of energy} \\ \text{added to the} \\ \text{system by mass} \\ \text{flow into the} \\ \text{system} \end{array} \right) \\
 &+ \left( \begin{array}{c} \text{Rate of energy} \\ \text{leaving} \\ \text{system by mass} \\ \text{flow out of} \\ \text{the system} \end{array} \right) + \left( \begin{array}{c} \text{Rate of} \\ \text{flow of heat} \\ \text{to the system} \\ \text{from the} \\ \text{surroundings} \end{array} \right) \quad (\text{B16})
 \end{aligned}$$

In the absence of shaft work the energy balance is (Fogler, 1992):

$$\begin{aligned}
 -K_{eff} A_r \frac{\partial T}{\partial r} \Big|_r + K_{eff} A_r \frac{\partial T}{\partial r} \Big|_{r+dr} + \sum_{j=1}^n N_j A_r H_j \Bigg|_r \\
 - \sum_{j=1}^n N_j A_r H_j \Bigg|_{r+dr} = \frac{\partial \left( \sum_{j=1}^n n_j U_j \right)}{\partial t} \quad j = 1, 2, \dots, n \\
 \quad i = 1, 2, \dots, m \quad (\text{B17})
 \end{aligned}$$

$U_j$  is internal energy component  $j$  in the system and  $H_j$  is enthalpy of component  $j$ , by considering the Taylor's extension, we have:

$$\begin{aligned}
 \frac{1}{A_r} \frac{\partial}{\partial r} \left( K_{eff} A_r \frac{\partial T}{\partial r} \right) - \frac{1}{A_r} \frac{\partial \left( \sum_{j=1}^n N_j A_r H_j \right)}{\partial r} \\
 = \frac{1}{A_r \times dr} \sum_{j=1}^n n_j \frac{\partial U_j}{\partial t} + \frac{1}{A_r \times dr} \sum_{j=1}^n U_j \frac{\partial n_j}{\partial t} \quad (\text{B18})
 \end{aligned}$$

Substituting Eq. (B5) in the above equation obtains:

$$\begin{aligned}
 \frac{1}{A_r} \frac{\partial}{\partial r} \left( K_{eff} A_r \frac{\partial T}{\partial r} \right) - \frac{1}{A_r} \sum_{j=1}^n H_j \frac{\partial (N_j A_r)}{\partial r} - \sum_{j=1}^n N_j \frac{\partial H_j}{\partial r} \\
 = \varepsilon \sum_{j=1}^n C_j \frac{\partial U_j}{\partial t} + \varepsilon \sum_{j=1}^n U_j \frac{\partial C_j}{\partial t} \quad (\text{B19})
 \end{aligned}$$

The term  $\frac{\partial (N_j A_r)}{\partial r}$  is replaced from Eq. (B8):

$$\begin{aligned}
 \frac{1}{A_r} \frac{\partial}{\partial r} \left( K_{eff} A_r \frac{\partial T}{\partial r} \right) + \sum_{j=1}^n H_j \left( -\rho_b \sum_{i=1}^m a_i \times v_{ij} r_i + \varepsilon \frac{\partial C_j}{\partial t} \right) \\
 - \sum_{j=1}^n N_j \frac{\partial H_j}{\partial r} \\
 = \varepsilon \sum_{j=1}^n C_j \frac{\partial U_j}{\partial t} + \varepsilon \sum_{j=1}^n U_j \frac{\partial C_j}{\partial t} \quad (\text{B20})
 \end{aligned}$$

Hence:

$$\begin{aligned}
 \frac{1}{A_r} \frac{\partial}{\partial r} \left( K_{eff} A_r \frac{\partial T}{\partial r} \right) - \sum_{j=1}^n H_j \left( \rho_b \sum_{i=1}^m a_i \times v_{ij} r_i \right) + \sum_{j=1}^n H_j \times \varepsilon \frac{\partial C_j}{\partial t} \\
 - \sum_{j=1}^n N_j \frac{\partial H_j}{\partial r} = \varepsilon \sum_{j=1}^n C_j \frac{\partial U_j}{\partial t} + \varepsilon \sum_{j=1}^n U_j \frac{\partial C_j}{\partial t} \quad (\text{B21})
 \end{aligned}$$

Now we have:

$$\begin{aligned}
 \frac{1}{A_r} \frac{\partial}{\partial r} \left( K_{eff} A_r \frac{\partial T}{\partial r} \right) - \rho_b \left( \sum_{i=1}^m \sum_{j=1}^n (H_j v_{ij}) \times a_i \times r_i \right) \\
 - \sum_{j=1}^n N_j \frac{\partial H_j}{\partial r} = \varepsilon \sum_{j=1}^n C_j \frac{\partial U_j}{\partial t} + \varepsilon \sum_{j=1}^n (U_j - H_j) \frac{\partial C_j}{\partial t} \quad (\text{B22})
 \end{aligned}$$

By using the following definitions, the last equation can be simplified:

$$\Delta H_i = \sum_{j=1}^n (v_{ij} H_j) \quad (\text{B23})$$

$$\frac{\partial H_j}{\partial r} = \frac{\partial H_j}{\partial T} \times \frac{\partial T}{\partial r} = C_{Pj} \times \frac{\partial T}{\partial r} \quad (\text{B24})$$

$$\begin{aligned}
 \sum_{j=1}^n N_j \frac{\partial H_j}{\partial r} &= \sum_{j=1}^n ((J_j + C_j u_r) \times C_{Pj} \times \frac{\partial T}{\partial r}) \\
 &= \frac{\partial T}{\partial r} \sum_{j=1}^n ((J_j + C_j u_r) \times C_{Pj}) \simeq u_r \left( \sum_{j=1}^n C_j C_{Pj} \right) \frac{\partial T}{\partial r} \quad (\text{B25})
 \end{aligned}$$

$$\left( \sum_{j=1}^n C_j C_{Pj} \right) = C_T \left( \sum_{j=1}^n \left( \frac{C_j}{C_T} \right) C_{Pj} \right) = C_T \sum_{j=1}^n y_j C_{Pj} = C_T C_P \quad (\text{B26})$$

$$(U_j - H_j) = -Pv_j = -RT \quad (\text{B27})$$

$$\sum_{j=1}^n (U_j - H_j) \frac{\partial C_j}{\partial t} = -RT \sum_{j=1}^n \frac{\partial C_j}{\partial t} = -RT \frac{\partial C_T}{\partial t} \quad (\text{B28})$$

$$\frac{\partial U_j}{\partial t} = \frac{\partial U_j}{\partial T} \times \frac{\partial T}{\partial t} = C_{Vj} \times \frac{\partial T}{\partial t} \quad (\text{B29})$$

$$C_{Vj} = C_{Pj} - R \quad (\text{B30})$$

$$C_V = C_P - R \quad (\text{B31})$$

Also:

$$\sum_{j=1}^n C_j \frac{\partial U_j}{\partial t} = \sum_{j=1}^n C_j C_{Vj} \times \frac{\partial T}{\partial t} = \frac{\partial T}{\partial t} \sum_{j=1}^n C_j C_{Vj} = \left( \sum_{j=1}^n C_j C_{Vj} \right) \frac{\partial T}{\partial t} \quad (\text{B32})$$

$$\left( \sum_{j=1}^n C_j C_{Vj} \right) = C_T \left( \sum_{j=1}^n \left( \frac{C_j}{C_T} \right) C_{Vj} \right) = C_T \sum_{j=1}^n y_j C_{Vj} = C_T C_V \quad (\text{B33})$$

In the above equations,  $C_V$  and  $C_P$  are the average heat capacities of mixture at constant volume and pressure, respectively. Thus, by applying these auxiliary equations, we have:

$$\frac{1}{A_r} \frac{\partial}{\partial r} (K_{eff} A_r \frac{\partial T}{\partial r}) - \rho_b (\sum_{i=1}^m \Delta H_i \times a_i \times r_i) - u_r C_T C_P \frac{\partial T}{\partial r} = \varepsilon C_T C_V \frac{\partial T}{\partial t} - \varepsilon R T \frac{\partial C_T}{\partial t} \quad (B34)$$

And then,

$$\frac{1}{A_r} \frac{\partial}{\partial r} (K_{eff} A_r \frac{\partial T}{\partial r}) - \rho_b (\sum_{i=1}^m \Delta H_i \times a_i \times r_i) - u_r C_T C_P \frac{\partial T}{\partial r} + \varepsilon R T \frac{\partial C_T}{\partial t} = \varepsilon C_T C_V \frac{\partial T}{\partial t} \quad (B35)$$

Due to steady state conditions and low amount of conductive heat transfer in comparison with convective heat transfer, therefore, heat transfer simplify to:

$$-u_r C_T C_P \frac{\partial T}{\partial r} - \rho_b \sum_{i=1}^m (\Delta H_i \times a_i \times r_i) = 0 \quad (B36)$$

Consequently, final equation for energy balance in the CCR process obtains:

$$\frac{\partial T}{\partial r} = -\frac{\rho_b}{u_r C_T C_P} \sum_{i=1}^m (\Delta H_i \times a_i \times r_i) \quad (B37)$$

### Appendix C. Collector equations

To represent the governing equations in the collector, mass and energy balances have been applied for a control volume with length of  $dz$  and cross section area of  $\pi R_i^2$ , thus, the mass balance for control element in  $Z$  direction is:

$$F_j|_z - F_j|_{z+dz} + F_{je} = 0 \quad (C1)$$

where  $F_j$  is molar flow rate of component  $j$  in  $Z$  direction and  $F_{je}$  is output molar flow rate of component  $j$  from reaction side that enters to the collector:

$$F_{je} = C_{je} u_{re} A_{re} = C_{je} u_{re} 2\pi R_i \times dz \quad (C2)$$

where  $C_{je}$  and  $u_{re}$  are concentration of component  $j$  and radial velocity in inner radius of reactor. By substituting recent equation in Eq. (C1), final equation for mass balance in the collector obtains:

$$\frac{\partial F_j}{\partial z} = 2\pi R_i u_{re} C_{je} \quad (C3)$$

Then, to calculate total molar flow rate  $F_T$ , the summation of recent equation for all pseudo-components must be considered:

$$\sum_{j=1}^n \frac{\partial F_j}{\partial z} = \sum_{j=1}^n (2\pi R_i u_{re} C_{je}) \quad (C4)$$

$$\sum_{j=1}^n \frac{\partial F_j}{\partial z} = 2\pi R_i u_{re} \sum_{j=1}^n (C_{je}) \quad (C5)$$

$$\frac{\partial F_T}{\partial z} = 2\pi R_i \times u_{re} \times C_{Te} \quad (C6)$$

Also, energy balance in the  $Z$  coordinates for a control volume is:

$$F_T C_P T|_z - F_T C_P T|_{z+dz} + \sum_{j=1}^n F_{je} C_{P_{je}} (T_e - T) = 0 \quad (C7)$$

Then, following definitions are used to simply the recent equation:

$$F_T = \sum_{j=1}^n F_j \quad (C8)$$

$$M = \frac{\sum_{j=1}^n M_j F_j}{F_T} \quad (C9)$$

$$C_p = \frac{\sum_{j=1}^n F_j C_{pj}}{F_T} \quad (C10)$$

$$\sum_{j=1}^n (C_{je} C_{P_{je}}) = C_{Te} \sum_{j=1}^n ((\frac{C_{je}}{C_{Te}}) C_{P_{je}}) = C_{Te} \sum_{j=1}^n (y_{je} C_{P_{je}}) = C_{Te} C_{Pe} \quad (C11)$$

By substituting the above equation in governing energy balance:

$$F_T C_P T|_z - F_T C_P T|_{z+dz} + \sum_{j=1}^n C_{je} u_{re} 2\pi R_i \times dz \times C_{P_{je}} (T_e - T) = 0 \quad (C12)$$

By writing the first and second terms of Taylor's extension in left hand of equation, ones can obtain:

$$\frac{\partial (F_T C_P T)}{\partial z} = 2\pi R_i \times u_{re} \times C_{Te} \times C_{Pe} \times (T_e - T) \quad (C13)$$

Now, by applying algebraic definitions Eq. (C13) simplifies:

$$C_P T \frac{\partial (F_T)}{\partial z} + F_T C_P \frac{\partial (T)}{\partial z} + F_T T \frac{\partial (C_P)}{\partial z} = 2\pi R_i \times u_{re} \times C_{Te} \times C_{Pe} \times (T_e - T) \quad (C14)$$

$$\frac{1}{T} \frac{\partial T}{\partial z} + \frac{1}{C_P} \frac{\partial C_P}{\partial z} + \frac{1}{F_T} \frac{\partial F_T}{\partial z} = \frac{1}{F_T C_P T} \times 2\pi R_i \times u_{re} \times C_{Te} \times C_{Pe} \times (T_e - T) \quad (C15)$$

And by rearranging Eq. (C15) we have:

$$\frac{\partial T}{\partial z} = -\frac{T}{C_p} \frac{\partial C_p}{\partial z} - \frac{T}{F_T} \frac{\partial F_T}{\partial z} + \frac{1}{F_T C_p} \times 2\pi R_i \times u_{re} \times C_{Te} \times C_{pe} \times (T_e - T) \quad (C16)$$

Then by substituting Eq. (C6) in the recent equation we have:

$$\frac{\partial T}{\partial z} = -\frac{T}{C_p} \frac{\partial C_p}{\partial z} - \frac{T}{F_T} (2\pi R_i \times u_{re} \times C_{Te}) + \frac{1}{F_T C_p} \times 2\pi R_i \times u_{re} \times C_{Te} \times C_{pe} \times (T_e - T) \quad (C17)$$

## Appendix D. Velocity distribution

For velocity distribution by using mass balance in the CCR process

$$\frac{\partial C_j}{\partial r} = -\frac{C_j}{r} - \frac{C_j}{u_r} \frac{\partial u_r}{\partial r} + \frac{\rho_b}{u_r} \sum_{i=1}^m a_i \times v_{ij} r_i \quad j = 1, 2, \dots, n \quad (D1)$$

Then the summation of recent equation for all pseudo-components must be calculated

$$\sum_{j=1}^n \frac{\partial C_j}{\partial r} = \sum_{j=1}^n -\frac{C_j}{r} - \frac{1}{u_r} \frac{\partial u_r}{\partial r} \sum_{j=1}^n C_j + \frac{\rho_b}{u_r} \sum_{j=1}^n \sum_{i=1}^m a_i \times v_{ij} r_i \quad (D2)$$

$$\frac{\partial C_T}{\partial r} = -\frac{C_T}{r} - \frac{C_T}{u_r} \frac{\partial u_r}{\partial r} + \frac{\rho_b}{u_r} \sum_{j=1}^n \sum_{i=1}^m a_i \times v_{ij} r_i \quad (D3)$$

$$\frac{u_r}{C_T} \times \frac{\partial C_T}{\partial r} = -\frac{u_r}{r} - \frac{\partial u_r}{\partial r} + \frac{\rho_b}{C_T} \sum_{j=1}^n \sum_{i=1}^m a_i \times v_{ij} r_i \quad (D4)$$

By rearranging Eq. (D4) velocity distribution equation can be obtained:

$$\frac{\partial u_r}{\partial r} = -\frac{u_r}{r} - \frac{u_r}{C_T} \times \frac{\partial C_T}{\partial r} + \frac{\rho_b}{C_T} \sum_{j=1}^n \sum_{i=1}^m a_i \times v_{ij} r_i \quad (D7)$$

To find  $\frac{\partial C_T}{\partial r}$  in the recent equation, we can use ideal gas law:

$$C_T = \frac{P}{RT} \quad (D8)$$

Then by doing algebraic operations on the above relations, we have:

$$\frac{\partial C_T}{\partial r} = \frac{1}{RT} \frac{\partial P}{\partial r} - \frac{P}{RT^2} \frac{\partial T}{\partial r} \quad (D9)$$

## References

- Aitani, A.M., 2005a. Catalytic naphtha reforming. In: Encyclopedia of Chemical Processing, <http://dx.doi.org/10.1081/E-ECHP-120039766>.
- Aitani, A.M., 2005b. *Catalytic Naphtha Reforming. Science and Technology*. Marcel Dekker, New York.
- Antos, G.A., Aitani, A.M., 1995. Catalytic naphtha reforming, 2nd ed. Marcel Dekker, New York.
- Barbier, J., 1986. Deactivation of reforming catalysts by coking—a review. *Appl. Catal.* 23, 225–243.
- Bishara, A., Stanislaus, A., Hussain, S., 1984. Effect of feed composition and operating conditions on catalyst deactivation and on product yield and quality during naphtha catalytic reforming. *Appl. Catal.* 13, 113–125.
- Carter, J.L., McVicker, G.B., Weissman, W., Kmaka, M.S., Sinfelt, J.H., 1982. Bimetallic catalysis; application in catalytic reforming. *Appl. Catal.* 3, 327–346.
- Edgar, M.D., 1983. Catalytic reforming of naphtha in petroleum refineries. In: *Applied Industrial Catalysis*. Academic Press, New York, pp. 1–123.
- Figoli, N.S., Beltramini, J.N., Barra, A.F., Martinelli, E.E., Sad, M.R., Parera, J.M., 1983a. Influence of total pressure and hydrogen: hydrocarbon ratio on coke formation over naphtha-reforming catalyst. In: *Coke Formation on Metal Surfaces ACS Symp. Ser.*, vol. 202, pp. 239–252.
- Figoli, N.S., Beltramini, J.N., Marinelli, E.E., Sad, M.R., Parera, J.M., 1983b. Operational conditions and coke formation on Pt-Al<sub>2</sub>O<sub>3</sub> reforming catalyst. *Appl. Catal.* 5, 19–32.
- Fogler, H.S., 1992. *Elements of Chemical Reaction Engineering*, 2nd ed. Prentice-Hall, Englewood Cliffs, NJ.
- Froment, G.B., 1987. The kinetic of complex catalytic reactions. *Chem. Eng. Sci.* 42, 1073–1087.
- Hongjun, Z., Mingliang, S., Huixin, N., Zeji, L., Hongbo, J., 2010. Modeling and simulation of moving bed reactor for catalytic naphtha reforming. *Petrol. Sci. Technol.* 28, 667–676.
- Hu, Y.Y., Su, H.Y., Chu, J., 2003. Modeling and simulation of commercial catalytic reformers. *Chin. J. Chem. Eng.* 17, 418–424.
- Iranshahi, D., Bahmanpour, A.M., Pourazadi, E., Rahimpour, M.R., 2010a. Mathematical modeling of a multi-stage naphtha reforming process using novel thermally coupled recuperative reactors to enhance aromatic production. *Int. J. Hydrogen Energy* 35, 10984–10993.
- Iranshahi, D., Pourazadi, E., Paymooni, K., Bahmanpour, A.M., Rahimpour, M.R., Shariati, A., 2010b. Modeling of an axial flow, spherical packed bed reactor for naphtha reforming process in the presence of the catalyst deactivation. *Int. J. Hydrogen Energy* 35, 12784–12799.
- Iranshahi, D., Pourazadi, E., Paymooni, K., Rahimpour, M.R., 2012. A novel dynamic membrane reactor concept with radial-flow pattern for reacting material and axial-flow pattern for sweeping gas in catalytic naphtha reformers. *AIChE J.* 58, 1230–1247.
- Iranshahi, D., Rahimpour, M.R., Asgari, A., 2010c. A novel dynamic radial flow, spherical-bed reactor concept for naphtha reforming in the presence of catalyst deactivation. *Int. J. Hydrogen Energy* 35, 6261–6275.
- Jenkins, J.H., Stephens, T.W., 1980. Kinetics of catalytic reforming. *Hydrocarb. Process.* 11, 163–167.
- Jorge, A.J., Eduardo, V.M., 2000. Kinetic modeling of naphtha catalytic reforming reactions. *Energy Fuels* 14, 1032–1037.
- Juarez, J.A., Macias, E.V., Garcia, L.D., Arredondo, E.G., 2001. Modeling and simulation of four catalytic reactors in series for naphtha reforming. *Energy Fuels* 15, 887–893.
- Kmak, W.S., 1972. A Kinetic simulation model of the powerforming process. AIChE Meeting, Houston, TX.
- Krane, H.G., Groh, A.B., Schuhnan, B.L., Sinfelt, J.H., 1959. Reactions in catalytic reforming of naphthas. In: *5th World Petroleum Congress*, New York, May 30–June 5.
- Lee, J.W., Ko, Y.C., Jung, Y.K., Lee, K.S., Yoon, E.S., 1997. A Modeling and simulation study on a naphtha reforming unit with a catalyst circulation and regeneration system. *Comput. Chem. Eng.* 21, 1105–1110.
- Lieske, H., Sarkany, A., Volter, J., 1987. Hydrocarbon adsorption and coke formation on Pt/Al<sub>2</sub>O<sub>3</sub> and Pt-Sn/Al<sub>2</sub>O<sub>3</sub> catalysts. *Appl. Catal.* 30, 69–80.
- Liu, K., Fung, S.C., Ho, T.C., Rumschitzki, D.S., 1997. Kinetics of catalyst coking in heptane reforming over Pt-Re/Al<sub>2</sub>O<sub>3</sub>. *Ind. Eng. Chem. Res.* 36, 3264–3274.
- Liu, K., Fung, S.C., Ho, T.C., Rumschitzki, D.S., 2002. Heptane reforming over Pt-Re/Al<sub>2</sub>O<sub>3</sub>: reaction network, kinetics, and apparent selective catalyst deactivation. *J. Catal.* 206, 188–201.
- Mahdavian, M., Shohreh, F., Fazeliz, A., 2010. Modeling and simulation of industrial continuous naphtha catalytic

- reformer accompanied with delumping the naphtha feed. *Int. J. Chem. React. Eng.* 8.
- Marin, G.B., Froment, G.B., Lerou, J.J., Backer, W.D., 1983. *Simulation of a catalytic naphtha reforming unit* W. Eur. Fed. Chem. Eng. 2, 1–7.
- Matar, S., Hatch, L.F., 2000. *Chemistry of Petrochemical Processes*, 2nd ed. Gulf Publishing Company, Texas.
- Mieville, R.L., 1991. Coking kinetics of reforming. *Stud. Surf. Sci. Catal.* 68, 151–159.
- Mostafazadeh, A.K., Rahimpour, M.R., 2009. A membrane catalytic bed concept for naphtha reforming in the presence of catalyst deactivation. *Chem. Eng. Process.* 48, 683–694.
- Nauman, E.B., 2001. *Chemical Reactor Design, Optimization, and Scaleup*. McGraw-Hill, New York.
- Padmavathi, G., Chaudhuri, K.K., 1997. Modeling and simulation of commercial catalytic naphtha reformers. *Can. J. Chem. Eng.* 75, 930–937.
- Pisyorius, J.T., 1985. Analysis improves catalytic reformer troubleshooting. *Oil Gas J.* 23, 147–151.
- Rahimpour, M.R., 2009. Enhancement of hydrogen production in a novel fluidized-bed membrane reactor for naphtha reforming. *Int. J. Hydrogen Energy* 34, 2235–2251.
- Rahimpour, M.R., Iranshahi, D., Pourazadi, E., Paymooni, K., Bahmanpour, A.M., 2011. The aromatic enhancement in the axial-flow spherical packed-bed membrane naphtha reformers in the presence of catalyst deactivation. *AIChE J.* 57, 3182–3198.
- Ramage, M.P., Graziani, K.P., Krambeck, F.J., 1980. Development of mobil's kinetic reforming model. *Chem. Eng. Sci.* 35, 41–48.
- Ramage, M.P., Graziani, K.P., Schipper, P.H., Krambeck, F.J., Choi, B.C., 1987. A review of mobil's industrial process modeling philosophy. *Adv. Chem. Eng.* 13, 193–266.
- Roldán, R., Romero, F.J., Jiménez1, C., Borau, V., Marinas, J.M., 2004. Transformation of mixtures of benzene and xylenes into toluene by transalkylation on zeolites. *Appl. Catal. A* 266, 203–210.
- Smith, R.B., 1959. Kinetic analysis of naphtha reforming with platinum catalyst. *Chem. Eng. Prog.* 55, 76–80.
- Tailleur, R.G., Davila, Y., 2008. Optimal hydrogen production through revamping a naphtha-reforming unit: catalyst deactivation. *Energy Fuels* 22, 2892–2901.
- Taskar, U., Riggs, J.B., 1997. Modeling and optimization of a semiregenerative catalytic naphtha reformer. *AIChE J.* 43, 740–753.
- Weifeng, H., Hongye, S., Yongyou, H., Jian, C., 2006. Modeling, simulation and optimization of a whole industrial catalytic naphtha reforming process on Aspen Plus platform. *Chin. J. Chem. Eng.* 14, 584–591.
- Weifeng, W., Hongye, S., Shengjing, M., Jian, C., 2007. Multi objective optimization of the industrial naphtha catalytic reforming process. *Chin. J. Chem. Eng.* 15, 75–80.
- Wolff, A., Kramarz, J., 1979. Kinetic models of catalytic reforming. *Chem. Technol. Fuels Oils* 15, 870–877.

## Further reading

- Perry, R.H., Green, D.W., Maloney, J.O., 1999. *Perry's Chemical Engineers' Handbook*, 7th ed. McGraw-Hill, New York.